Received: 8 November 2017 | Revised: 7 February 2018 | Accepted: 13 February 2018
DOI: 10.1002/ardp.201700349

FULL PAPER

DPhG ARCH PHARM
Archiv der Pharmazie

Non-peptide-based new class of platelet aggregation inhibitors: Design, synthesis, bioevaluation, SAR, and *in silico* studies

Pradeep K. Jaiswal[1] | **Vashundhra Sharma**[1] | **Surendra Kumar**[2] | **Manas Mathur**[3] | **Ajit K. Swami**[3] | **Dharmendra K. Yadav**[2,4] | **Sandeep Chaudhary**[1]

[1] Laboratory of Organic and Medicinal Chemistry, Department of Chemistry, Malaviya National Institute of Technology, Jaipur, India

[2] College of Pharmacy, Gachon University of Medicine and Science, Incheon City, Korea

[3] Department of Advance Molecular Microbiology, Seminal Applied Sciences Pvt. Ltd., Jaipur, India

[4] Department of Biochemistry, All India Institute of Medical Sciences (AIIMS), Jodhpur, Rajasthan, India

Correspondence
Prof. Sandeep Chaudhary, Laboratory of Organic and Medicinal Chemistry, Department of Chemistry, Malaviya National Institute of Technology, Jawaharlal Nehru Marg, Jaipur-302017, India.
Email: schaudhary.chy@mnit.ac.in

Dr. Dharmendra K. Yadav, College of Pharmacy, Gachon University of Medicine and Science, Incheon City-21936, Korea.
Email: dharmendra30oct@gmail.com

Funding information
National Research Foundation of Korea (NRF), Grant number: 2017R1C1B2003380; SERB, New Delhi for Fast Track Scheme for Young Scientist, Grant number: CS-037/2013; DST-RFBR Indo-Russian Joint Research Project, Grant number: INT/RUS/RFBR/P-169; CSIR-EMR Grant, New Delhi, Grant number: 02 (0189)/14/EMR-II

Abstract

A series of 2-oxo-2-phenylethylidene linked 2-oxo-benzo[1,4]oxazine analogues **17a–x** and **18a–o**, incorporated with a variety of electron-withdrawing as well as electron-donating groups at ring A and ring C, were synthesized under greener conditions in excellent yields (up to 98%). These analogues **17a–x** and **18a–o** were evaluated for their arachidonic acid (AA)-induced platelet aggregation inhibitory activities in comparison with the standard reference aspirin (IC_{50} = 21.34 ± 1.09 μg/mL). Among all the screened compounds, eight analogues, **17i**, **17x**, **18f**, **18g**, **18h**, **18i**, **18l**, and **18o**, were identified as promising platelet aggregation inhibitors as compared to aspirin. In addition, cytotoxic studies in $3T_3$ fibroblast cell lines by MTT assay of the promising compounds (**17i**, **17x**, **18f–18i**, **18l**, and **18o**) were also performed and the compounds were found to be non-toxic in nature. Furthermore, the results on the AA-induced platelet aggregation inhibitory activities of these compounds (**17i**, **17x**, **18f–18i**, **18l**, and **18o**) were validated via *in silico* molecular docking simulation studies. To the best of our knowledge, this is the first report of the identification of non-peptide-based functionalized 2-oxo-benzo[1,4]oxazines as platelet aggregation inhibitors.

KEYWORDS
2-oxo-benzo[1,4]oxazine, cytotoxicity, *in silico* molecular docking, platelet aggregation inhibitors, structure–activity relationship

1 | INTRODUCTION

Platelet aggregation, which causes thrombosis, represents one of the most important causes of cerebral stroke and arterial thromboembotic diseases, such as ischemic stroke, myocardial infarction, angina pectoris, and other cardiovascular diseases; and is responsible for morbidity and mortality in developing countries.[1,2] Primarily, platelet aggregation is a vital process in hemostasis formation which is being activated by the enzyme thrombin and transforms the fibrinogen (insoluble) into fibrin (soluble). It was firstly reported by Coller[3] (1960)

Pradeep K. Jaiswal and Vashundhra Sharma contributed equally to this paper.

that the platelet aggregation inhibitors might be the rationale for antithrombotic therapy. Anti-thrombotic therapy, which represents the treatment of thrombin platelet and thrombosis, are divided into three categories: (1) anti-platelet drugs (such as aspirin, ticlopidine, and indomethacin)[4]; (2) anti-coagulants or thrombin inhibiting drugs (such as heparin and warfarin)[5]; and (3) thrombolytic drugs (such as fibrin receptor antagonists).[6] Based on the mode of action, type 1 category, i.e., platelet aggregation inhibitors can be further sub-divided into three classes: (1) agents affecting arachidonic acid metabolism; (2) platelet activation factor (PAF) receptor antagonists; and (3) agents affecting ADP-dependent platelet aggregation pathway.[7]

The most clinically used anti-platelet drugs are either phosphodiesterase inhibitor/ADP receptor antagonists, or cyclooxygenase (COX) inhibitor as well as GpIIb/IIIa receptor antagonist.[8] Arachidonic acid (AA) is a fatty acid, which is liberated from the activated platelets and is converted into a potent inducer of platelet aggregation by the enzyme cyclooxyenase.[9] On the other hand, AA is also a precursor for thromboxane A2 (TBXA2) synthesis, which can stimulate platelet aggregation after conversion to prostaglandin G1 and H2.[10] Thus, in the initial step, prostaglandin-endoperoxide synthase 1 (PTGS1; which is also known as cyclooxygenase-1) catalyses the transformation of AA into cyclic endoperoxide PG G2 and H2 and after that this PGG2 and PGH2 are converted into TBXA2 by TBXA synthase in platelets.[10] Therefore, the inhibition of cyclooxygenase-1 is an important target in the identification of novel platelet aggregation inhibitors.[11] As a result, several non-peptide mimics such as aspirin **1**, tirofiban **2**, ticlopidine **3**, clopidogrel **4**, sulfinpyrazone **5**, etc. have been developed as a potent inhibitors of platelet aggregation[12] (Figure 1).

In spite of the efficacy of platelet aggregation inhibitory effect, several antiplatelet agents have been withdrawn from the market as these are associated with serious drawbacks such as adverse side-effects, increased mortality rate, high toxicity, etc.[13] Therefore, the identification of potent and safe platelet aggregation inhibitors is of great interest to synthetic medicinal chemists.[14]

Benzoxazine class of compounds are endowed with a wide range of biological activities[15] such as anti-tumor,[15a] anti-inflammatory,[15b] anti-microbial,[15c] antifungal,[15d] COX-2 inhibitor,[15e] rennin inhibitor,[15f] and non-steroidal progesterone receptor agonists.[15g] Recently, Zuo and co-workers reported benz[1,4]oxazine-3-one derivatives as an efficient GPIIb/IIIa receptor antagonists and displayed promising platelet aggregation inhibiting activity.[8,16] Dudley et al.[17] reported that benz[1,4]oxazine-3-one derivatives are remarkable inhibitors of Xa factor. Jakobson et al.[18] identified 2-aryl substituted benz[1,3]oxazine-4-one class of compounds as inhibitors of the tissue factor/factor VIIa-induced activation of factor Xa and *in situ* activates the fibrin clot formation. Moreover, Kikelj et al.[19] and Ilaš et al.[20] had also identified benz[1,4]oxazines as glycoprotein IIb/IIIa antagonists. Further structure–activity relationship (SAR) study on benz[1,4]oxazine-3-ones revealed them to show promising thrombin inhibitory and fibrinogen receptor antagonist activity.[21]

Recent literature revealed that 2-phenyl-4-quinolones have been reported to show platelet aggregation inhibitory activity via COX-1 inhibitors. Moreover, several similar bioactive classes of compounds were reported to show promising platelet aggregation inhibitory activity such as functionalized 1,3-benzoxazines **6**,[22a–c] 2-morpholino substituted benzoxazines **7**,[22d] benz[1,4]oxazine-3-ones **8**,[16] functionalized quinolin-4(1*H*)-ones **9**,[22e,f] substituted coumarins **10**, etc.[22g] (Figure 2).

It has been well documented that 3-oxo-benz[1,4]oxazines analogues **8** displayed good ADP, collagen, and PAF-induced platelet aggregation inhibitory activity. However, the AA-induced platelet aggregation inhibiting activities of 3-oxo-benz[1,4]oxazines were less explored. Therefore, in our endeavor in search for novel bioactive heterocycles as new antiplatelet agents, we designed *prototype* 11, i.e., functionalized 2-oxo-benzo[1,4]oxazines incorporating subunits of **5**–**10** (Figure 2), and assessed their AA-induced platelet aggregation inhibiting activities with the anticipation that the 2-oxo-benz[1,4]-oxazines scaffold would also show promising inhibitory activity. So far, literature report revealed that there is no report available showing 2-oxo-benz[1,4]oxazines as platelet aggregation inhibitory activity.

Herein, we report the ultrasonic-assisted synthesis,[23] platelet aggregation inhibitory activity, SAR, and cytotoxic studies of a series of functionalized 2-oxo-benzo[1,4]oxazines **17a–x** and **18a–o**, respectively. We also report the validation of our activity results via *in silico* molecular docking simulation studies. Although compounds **17a–x**, **18a**,**b**, and **18i** have been prepared earlier by other routes[24]; however, for the first time, compound **17b**,**c**, **17g**, **17q**, **17s**,**t**, **17v**, **18a**,**b**, and **18i** have been prepared via "on water" ultrasound-assisted methodology. Interestingly, the antiplatelet aggregation activities of all the synthesized compounds (**17a**–**x** and **18a**–**o**) have never been reported. To the best of our knowledge, for the first time, 2-oxo-benzo[1,4]oxazines, **17a–x** and **18a–o**, have been identified as new class of AA-induced platelet aggregation inhibitors. In this study, aspirin was used as standard reference. In addition, the cytotoxic studies of active compounds (**17i**, **17x**, **18f–18i**, **18l**, and **18o**) using $3T_3$ fibroblast cell lines in MTT assay were also performed. We also report the validation of results via *in silico* molecular docking simulation studies of active compounds **17i**, **17x**, **18f–18i**, **18l**, and **18o**.

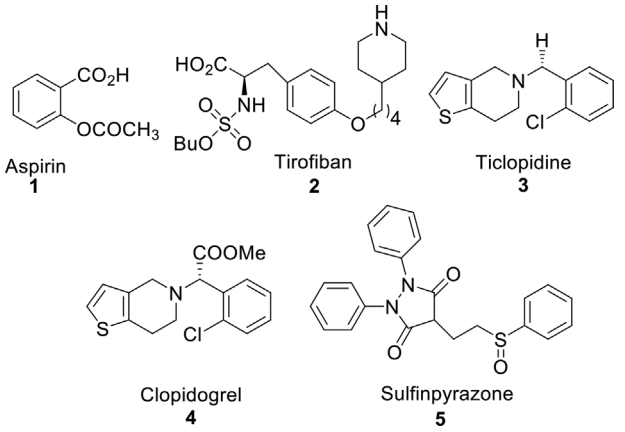

FIGURE 1 Structures of some clinically used platelet aggregation inhibitors

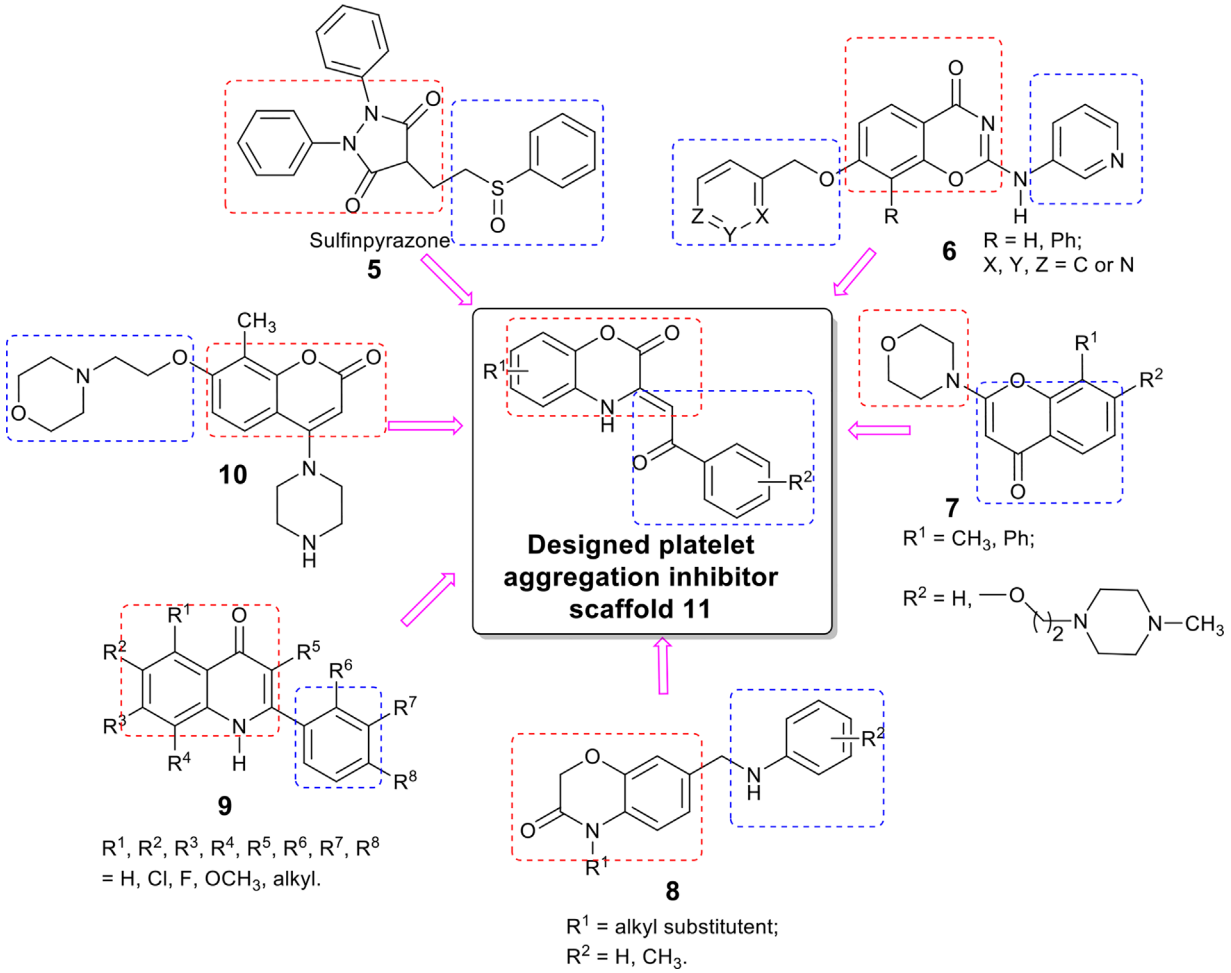

FIGURE 2 Design strategy for the target functionalized 3-(2-oxo-2-phenylethylidene)-3,4-dihydro-2*H*-benzo[*b*][1,4]oxazin-2-one as a new class of potential platelet aggregation inhibitors

2 | RESULTS AND DISCUSSION

2.1 | Chemistry

Recently, we reported two highly efficient, one pot, green methodologies for the synthesis of functionalized 2-oxo-benzo[1,4]oxazines under mild conditions.[23a,b] The "on water" ultrasonic-assisted[23a] methodology was utilized in the synthesis of a series of functionalized 2-oxo-benzo[1,4]oxazines **17a–x** and **18a–o** upto 98% yields. The required starting material for the synthesis of *prototype* **11** i.e., diketo-acids **15a–g** were synthesized in excellent yields (upto 92%) via base-catalyzed reaction of acetophenone **12a–g** with dimethyl oxalate **13** in toluene under refluxing condition for 6 h followed by the hydrolysis of resulting diketoesters **14a–g** with $LiOH.H_2O$ in MeOH/THF/H_2O (7:2:1; v/v) as solvents. While exploring target prototype **11**, we had observed that the reaction of nitro/alkyl/halide-substituted 2,4-dioxo-4-phenylbutanoic acid **15a–g** with nitro/alkyl/halide-substituted 2-aminophenol **16a–f** or **16e–g** in water furnished desired pure functionalized 2-oxo-benzo[1,4]oxazines **17a–x** and **18a–o** in excellent yields (up to 98%), respectively. The structures of all the synthesized compounds were confirmed by their spectral analysis (^{1}H NMR, ^{13}C NMR, FT-IR, and HRMS) (Scheme 1).

2.2 | Biological evaluation

2.2.1 | Platelet aggregation inhibitory activity evaluation

The generic structure of 2-oxo-benzo[1,4]oxazines is a bicyclic rings A & B having pendant substituted 2-oxo-phenylidene ring C (Table 1). Initially, we prepared 24 2-oxo-benzo[1,4]oxazines **17a–x** having various substituents at rings A and C, and evaluated for their arachidonic acid (AA) induced-antiplatelet aggregation inhibitory activities. In this study, the standard reference drug used was aspirin which showed IC_{50} values of 21.34 ± 1.09 μg/mL. As depicted from Table 1, out of all compounds, compounds such as **17i**, **17m**, **17s**, and **17x** having halogen atom at ring C showed promising inhibitory activities in comparison to the standard reference except compound **17k**. The model compound **17a**, which has no substitutions at ring A or

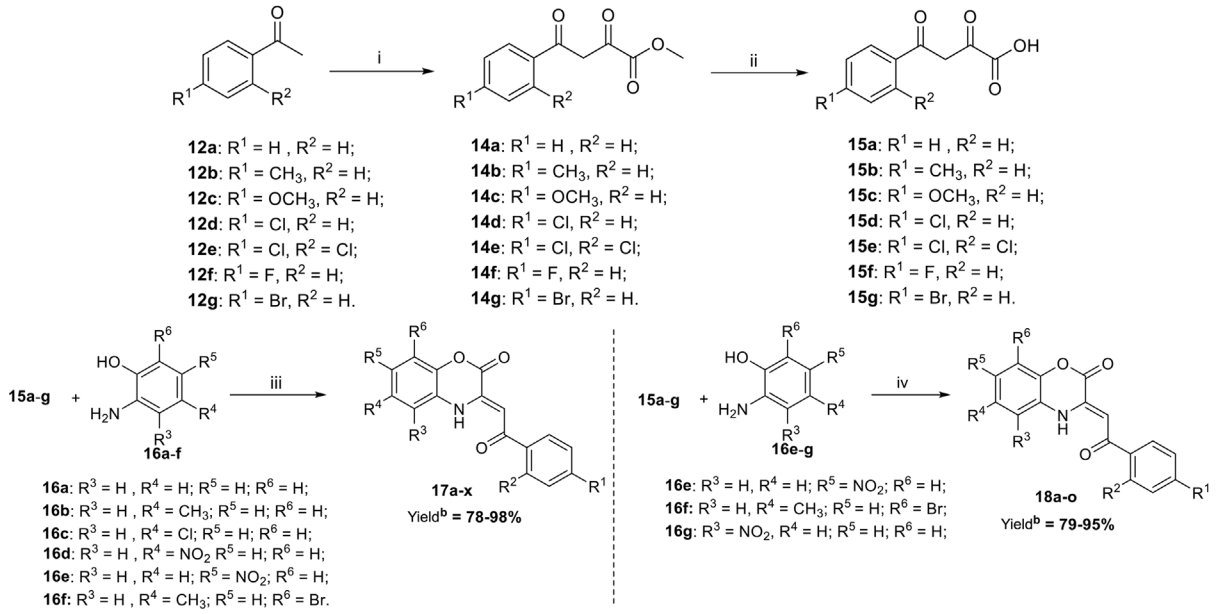

[a]*Reagents and conditions*: (i) **12a-g** (1.0 mmol), NaH (1.2 mmol), dimethyl oxalate **13** (1.0 mmol), toluene, 0–80°C, 5-6 h; (ii) **14a-g** (1.0 mmol), LiOH. H_2O (1.3 mmol), MeOH/THF/H_2O (15 ml; 7:2:1), 0°C to rt, 4-6 h; (iii) **15a-g** (0.2 mmol), **16a-f** (0.2 mmol), water (2.0 mL), ultrasound irradiation, 80°C, 75-120 min.; (iv) **15a-g** (0.2 mmol), **16e-g** (0.2 mmol), water (2.0 mL), ultrasound irradiation, 80°C, 75-120 min. [b]Isolated yield after column chromatography/recrystallization.

SCHEME 1 Ultrasound-assisted one-pot green synthesis of 2-oxo-benzo [1, 4]oxazines analogues (**17a–x** and **18a–o**)[a]

ring C, displayed more than two times lesser activity in comparison to the standard reference. Then, we synthesized compounds **17b–x** having various electron-withdrawing groups (EWG) as well as electron-donating groups (EDG) at ring A or ring C to interpret SAR studies with the anticipation that these substituents might cause an increase in the platelet aggregation inhibitory activity (Table 1).

Among all screened compounds, EDG (such as CH_3, Cl, Br, etc.) at ring A linked with EDG at ring C (compounds **17b–h** and **17j–o**; entry 2–8 and entry 10–15; Table 1) displayed lesser activity than aspirin. Whereas, the compound **17i** (IC_{50} = 22.87 ± 0.26 µg/mL; entry 9; Table 1), which has 3-methyl-6-bromo substituent at ring A and bromo substituent at ring B displayed comparable platelet aggregation inhibitory activity compared to aspirin. The compounds, which have EWG on 4- or 5-position at ring A (**17p–w**; entries 16–23; Table 1) exhibited lesser inhibitory activity than both drugs aspirin, except compound **17x** (IC_{50} = 19.74 ± 0.21 µg/mL; entry 24; Table 1), which has NO_2 EWG on 5-position at ring A, displayed better platelet aggregation inhibitory activity than standard drug aspirin. The promising compounds, **17i** and **17x**, found in our preliminary results prompted us to prepare further functionalized 2-oxo-benzo[1,4]-oxazines having similar variations.

Based on the structure of active compounds, **17i** and **17x**, and the preliminary biological results, we observed that the compounds having bromo substituent at ring C on 4-position and EDG (such as CH_3 and Br) on 3- and 6-position at ring A as well as EWG (such as NO_2) on 5-position at ring A were found to show potent platelet aggregation inhibitory activity. Therefore, a new series of functionalized 2-oxo-benzo[1,4]oxazines (**18a–o**; Scheme 1) incorporating different EWG and EDG at rings A and C were synthesized and assessed for their inhibitory antiplatelet aggregation activity (Table 2). The standard reference aspirin was analyzed again along with **18a–o**.

As it can be seen from Table 2, all the 15 compounds **18a–o** exhibited moderate to excellent anti-platelet aggregatory activities having IC_{50} values in the range of 17.96 ± 0.18–98.75 ± 1.46 µg/mL in comparison to the reference drug aspirin (IC_{50} = 21.59 ± 0.63). Compounds having EWG such as NO_2 at 5-position on ring A (**18a–d**; entry 1–4) having halo or methoxy group on ring C displayed lesser platelet aggregation inhibitory activity than aspirin. Whereas 6-Br and 4-Me groups at ring A along with F-, Cl-, OMe or CH_3-group on ring C i.e., compound **18e–h** (entry 5–8) were found to show either comparable platelet aggregation inhibiting activity (**18g** and **18h**; entry 7–8) or greater inhibitory activity (**18f**; entry 6) than aspirin. Moreover, while the compounds having EWG such as NO_2 at 3-position of ring A along with either no substitution (**18i**; entry 9) or EDG (such as Cl or Br) at 4-position of ring C (**18l** and **18o**; entry 12 and 15) displayed greater inhibitory activity than aspirin; compounds having CH_3-, OCH_3-, or F-groups exhibited lesser activity than aspirin. It is also noted that the compound having NO_2 EWG at ring A and 2,4-dichloro substituent on ring C (**18m**; entry 13) further decreases the inhibitory activity in comparison to the monochloro-substitution at ring A (**18l**; entry 12).

The SAR study indicates that the compounds with two EDG (i.e., 3-methyl-6-bromo substituted) at ring A along with X-group (X = Br, Cl) or OMe-group at ring C (i.e., **17i** and **18f–h**) displayed either equal inhibitory activity (as in **17i** and **18g**,**h**) or greater (**18f**) aggregation inhibitory activity than aspirin. In addition, the NO_2 EWG at 3-position (**18i**, **18l**, and **18o**) or 5-position (**17x**) on ring A along with either no substitution (**18i**) or X-group (X = Br, Cl) at 4-position

TABLE 1 *In vitro* AA-induced platelet aggregation inhibitory activity[22f] of a series of functionalized 2-oxobenzo[1,4]oxazines (**17a–x**)

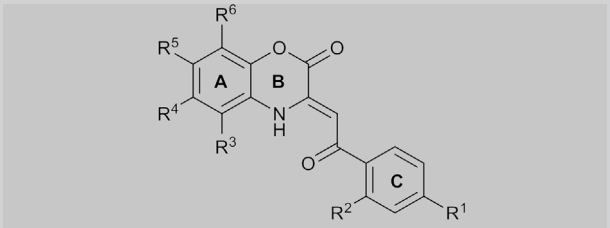

Generic structure of 2-oxo-benzo[1,4]oxazines

S. no.	Comp. no.	R^1	R^2	R^3	R^4	R^5	R^6	Antiplatelet activity[a,b] (IC_{50} in μg/mL)
1	**17a**	H	H	H	H	H	H	48.25 ± 0.71
2	**17b**	H	H	H	CH_3	H	H	94.67 ± 1.41
3	**17c**	CH_3	H	H	CH_3	H	H	85.21 ± 1.16
4	**17d**	OCH_3	H	H	CH_3	H	H	525 ± 3.41
5	**17e**	Cl	Cl	H	CH_3	H	H	95.4 ± 1.43
6	**17f**	F	H	H	CH_3	H	H	93.37 ± 1.38
7	**17g**	Br	H	H	CH_3	H	H	467 ± 2.89
8	**17h**	H	H	H	CH_3	H	Br	87.32 ± 0.96
9	**17i**	Br	H	H	CH_3	H	Br	**22.87 ± 0.26**
10	**17j**	H	H	H	Cl	H	H	92.94 ± 1.38
11	**17k**	CH_3	H	H	Cl	H	H	33.97 ± 0.54
12	**17l**	Cl	H	H	Cl	H	H	531 ± 3.44
13	**17m**	F	H	H	Cl	H	H	**30.11 ± 0.37**
14	**17n**	Br	H	H	Cl	H	H	91.23 ± 1.36
15	**17o**	OCH_3	H	H	Cl	H	H	473.45 ± 2.47
16	**17p**	H	H	H	NO_2	H	H	455.38 ± 2.28
17	**17q**	CH_3	H	H	NO_2	H	H	91.23 ± 1.36
18	**17r**	OCH_3	H	H	NO_2	H	H	88.23 ± 1.28
19	**17s**	Cl	H	H	NO_2	H	H	**28.12 ± 0.22**
20	**17t**	Cl	Cl	H	NO_2	H	H	87.03 ± 1.21
21	**17u**	F	H	H	NO_2	H	H	469.21 ± 2.31
22	**17v**	Br	H	H	NO_2	H	H	89.11 ± 1.27
23	**17w**	H	H	H	H	NO_2	H	84.21 ± 1.13
24	**17x**	Br	H	H	H	NO_2	H	**19.74 ± 0.21**
25	Aspirin	–	–	–	–	–	–	21.34 ± 1.09

The bold values indicate promising anti-platelet activity of compounds.

[a]Platelets were incubated along with either a tested compound or 0.5% DMSO at 37°C for 60 s, then AA (100 μM) was added to accelerate the aggregation. Aspirin was used as positive control. Values are expressed as mean ± SE from three to six separations.

[b]The data represent mean of three independent determinations.

on ring C (**18l** and **18o**) exhibited greater platelet aggregation inhibitory activity than aspirin.

2.2.2 | Cytoxicity evaluation[25]

Out of 39 compounds, 8 compounds i.e., **17i**, **17x**, **18f**, **18g**, **18h**, **18i**, **18l**, and **18o** (showing promising or greater potency) were selected for their cytotoxic studies using $3T_3$ fibroblast cell lines in MTT assay.[25] The result showed that these compounds were non-toxic to $3T_3$ fibroblast cell lines even at 250 μg/mL concentration and consequently displayed permissible values of cell viability (Figure 3).

2.3 | *In silico* molecular docking studies[26]

To study the binding modes of the eight molecules (**17i**, **17x**, **18f**, **18g**, **18h**, **18i**, **18l**, and **18o)** in the cyclooxygenase-1 (COX-1) enzyme, first

TABLE 2 *In vitro* AA-induced platelet aggregation inhibitory activity of a new series of functionalized 2-oxo-benzo[1,4]oxazines (**18a–o**)

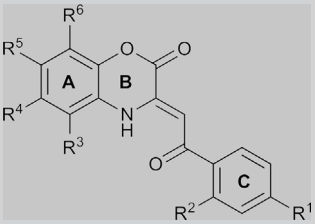

S. no.	Comp. no.	R^1	R^2	R^3	R^4	R^5	R^6	Antiplatelet activity [a,b] (IC_{50} in μg/mL)
1	**18a**	OCH_3	H	H	H	NO_2	H	82.35 ± 1.11
2	**18b**	Cl	H	H	H	NO_2	H	28.12 ± 0.22
3	**18c**	Cl	Cl	H	H	NO_2	H	98.75 ± 1.46
4	**18d**	F	H	H	H	NO_2	H	41.11 ± 0.47
5	**18e**	CH_3	H	H	CH_3	H	Br	45.97 ± 0.65
6	**18f**	OCH_3	H	H	CH_3	H	Br	**19.83 ± 0.22**
7	**18g**	Cl	Cl	H	CH_3	H	Br	**20.08 ± 0.24**
8	**18h**	F	H	H	CH_3	H	Br	**21.47 ± 0.24**
9	**18i**	H	H	NO_2	H	H	H	**16.96 ± 0.18**
10	**18j**	CH_3	H	NO_2	H	H	H	29.87 ± 0.30
11	**18k**	OCH_3	H	NO_2	H	H	H	36.54 ± 0.35
12	**18l**	Cl	H	NO_2	H	H	H	**19.19 ± 0.22**
13	**18m**	Cl	Cl	NO_2	H	H	H	41.35 ± 0.53
14	**18n**	F	H	NO_2	H	H	H	44.08 ± 0.64
15	**18o**	Br	H	NO_2	H	H	H	**17.96 ± 0.18**
16	Aspirin	–	–	–	–	–	–	21.59 ± 0.63

The bold values indicate promising anti-platelet activity of compounds.
[a]Platelets were incubated along with either a tested compound or 0.5% DMSO at 37°C for 60 s, then AA (100 μM) was added to accelerate the aggregation. Aspirin was used as positive control. Values are expressed as mean ± SE from three to six separations.
[b]The data represent mean of three independent determination.

we performed molecular docking study with reference standard compound aspirin on COX-1 domain (PDB ID: 2OYE) using Surflex-Dock. After running Surflex-Dock, the conformers were ranked in a molecular spread sheet based on their docking scores, and the best docked score conformers were selected, and speculated concerning the detailed binding mode in the active site.[26e,f] A docking score represents binding affinity, which include hydrophobic, repulsive, entropic, polar, and solvation. The docking results for **18i** and **18o** against the antiplatelet target COX-1 showed a high binding affinity

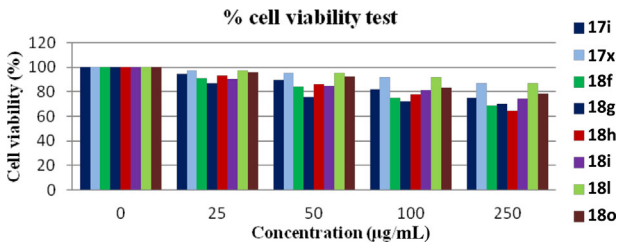

FIGURE 3 Percentage cell viability test

docking score indicated by a total score of 5.5546 and 5.7941, respectively, forms a H-bond of length 1.7 and 2.3 Å to the side chain of nucleophilic (polar, hydrophobic) residue i.e., Ser-530. In the docking pose of compound **18i** and **18o**-COX-1 complex, the chemical nature of binding site residues within a radius of 4 Å was aromatic (hydrophobic), for example, Phe-381, Phe-518, Trp-387, Tyr-385, Tyr-348; nucleophilic (polar, hydrophobic) residue Ser-353; hydrophobic, for example, Val-349, Ala-527, Gly-526, Ile-523, Leu-352, and Met-522; as a result, the bound compound showed a strong hydrophobic interaction with COX-1, thus leading to more stability and activity in this compound (predicted interactions of **18i** (4A) and **18o** (4B) with antiplatelet target enzyme COX-1, as given in Figure 4A and B).

On the other hand, docking results for compound **18g** and **18l** against the target protein COX-1 showed a high binding affinity docking score indicated by a total score of 4.5281 and 4.4766, respectively, forms a salt bridge of length 4.6 Å to the polar, hydrophobic, positive-charged residue Arginine-120. In the docking pose of the complex, the chemical nature of binding site residues

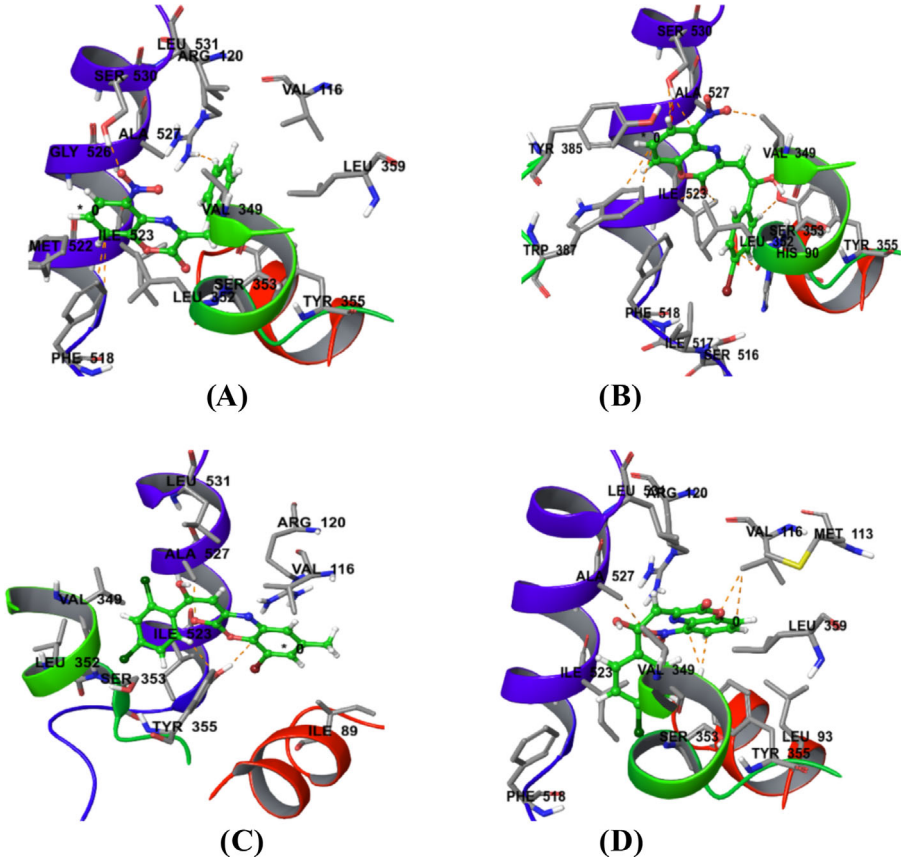

FIGURE 4 (A and B) Predicted interactions of **18i** (A) and **18o** (B) with antiplatelet target enzyme COX-1 (PDB: 2OYE) with a docking total score of 5.5546 and 5.7941, respectively, revealing H-bonds of length 1.7 and 2.3, respectively, to the binding site pocket residues Ser-530. (C and D) Predicted interactions of **18g** (C) and **18l** (D) with antiplateles target enzyme COX-1 (PDB: 2OYE) with a docking total score of 4.5281 and 4.4766, respectively, revealing a salt bridge of length 4.6, to the binding site pocket residues Arg-120

within a radius of 4 Å was acidic (polar, negative charged), for example, Glu-524; hydrophobic, for example, Val-116, Val-349, Ala-527, Ile-89, Ile-523, Leu-93, Leu-531, Leu-359, Leu-352, and Met-113; nucleophilic (polar, hydrophobic) residue Ser-530, Ser-353; and aromatic (hydrophobic), for example, Phe-518, Tyr-355; as a result, the bound compound showed a strong hydrophobic interaction with COX-1, thus leading to more stability and activity in this compound (predicted interactions of **18g** (4C) and **18l** (4D) with antiplatelet target enzyme COX-1, as shown in Figure 4C and D).

Likewise, docking results for compound **17i** and **17x** against the target protein COX-1 showed a high binding affinity docking score indicated by a total score of 4.9098 and 4.9098, respectively, forms a H-bond of length 1.8 and 2.7 Å to the side chain of hydrophobic aromatic residue that is, Phen-518 and nucleophilic (polar, hydrophobic) residue that is, Ser-553. On the other hand, docking results for **17x** formed a π-cation interaction with side chain of Tyr-385, —NH^+ atom of pyridine ring formed π-cation with —H atom of OH group of Tyr-385 (pyridine-NH^+...OH, Tyr-385, 3.9 Å). In the docking pose of the complex, the chemical nature of binding site residues within a radius of 4 Å was basic (polar, hydrophobic, positive charged), for example, Arg-120; acidic (polar, negative charged), for example, Glu-524; aromatic (hydrophobic), for example, Tyr-355; hydrophobic, for example, Leu-359, Leu-531, Leu-352, Leu-93, Met-113, Ala-527, Ile-523, Ile-89, Val-349, Val-116, as a result, the bound compound showed a strong hydrophobic interaction with COX-1, thus leading to more stability and significant activity in this compound (predicted interactions of **17i** (5A) and **17x** (5B) with antiplatelet target enzyme COX-1, as shown in Figure 5A and B).

Moreover, the docking results for compound **18f** and **18h** against the target protein COX-1 showed a high binding affinity docking score indicated by a total score of 5.6388 and 4.5653, respectively. Compound **18f** formed a π–π stacking with of Tyr-385, —Cl atom of pyridine ring formed π–π stacking with —OH group of Tyr-385 (pyridine-Cl...OH, Tyr-385, 5.3 Å), and Tyr-355 —F atom of pyridine ring —OH group of Tyr-355 (pyridine-F...OH, Tyr-355, 5.4 Å). In the docking pose of the complex, the chemical nature of binding site residues within a radius of 4 Å was hydrophobic, for example, Leu-352, Leu-359, Leu-531, Ala-527, Val-349, Val-116, Ile-523; polar amide type, for example, His-90; aromatic (hydrophobic), for example, Tyr-355; nucleophilic (polar, hydrophobic) residue that is, Ser-353, Ser-530; positive charged), for example, Arg-120; as a result, the bound compound showed a strong hydrophobic interaction with COX-1, thus

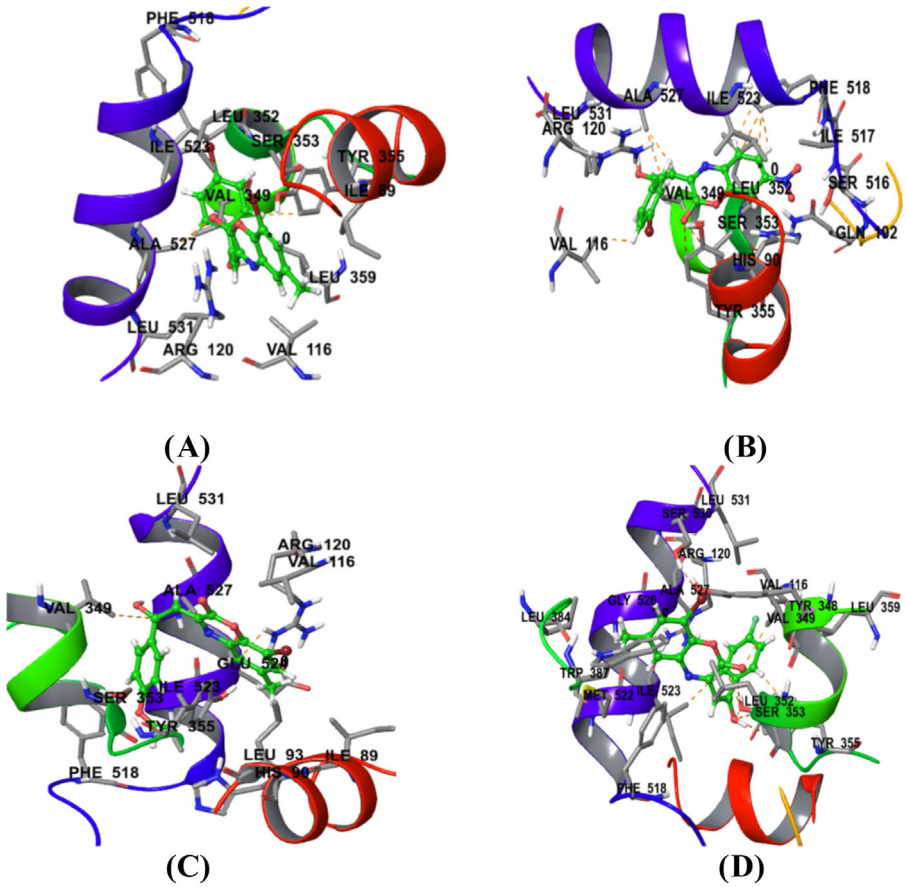

FIGURE 5 (A and B) Predicted interactions of **17i** (A) and **17x** (B) with antiplatelet target enzyme COX-1 (PDB: 2OYE) with a docking total score of 4.9098 and 4.9098, respectively, revealing H-bonds of length 1.8 and 2.7, to the binding site pocket residues Phen-518 and Ser-553, respectively. (C and D) Predicted interactions of **18f** (C) and **18h** (D) with antiplatelet target enzyme COX-1 (PDB: 2OYE) with a docking total score of 5.6388 and 4.5653, respectively, revealing π–π stacking of length 5.3 and 5.4, to the binding site pocket residues Tyr-385 and Tyr-355, respectively

leading to more stability and significant activity in this compound (predicted interactions of **18f** (5C) and **18h** (5D) with antiplatelet target enzyme COX-1, as shown in Figure 5C and D).

Furthermore, the docking result for the reference drug aspirin with the antiplatelet target protein COX-1 showed a low binding affinity docking score, indicated by a low total score of 4.4422 and forms a H-bond of length 1.8 Å to the side chain of basic (polar, hydrophobic, positive charged), for example, Arg-120 (predicted interactions of aspirin with antiplatelet target enzyme COX-1, as shown in Figure 6). Thus, the docking procedure of Surflex-Dock software (Sybyl-X 2.1) in reproducing the experimental binding affinity seems reliable, and therefore predicted as true positive.

After docking analysis, it has been observed that the most active 2-oxo-benzo[1,4]oxazines, **18i** (IC_{50} = 16.96 ± 0.18) and **18o** (IC_{50} = 17.96 ± 0.18), showed strong interaction at Ser-530 binding site pocket residues (docking total score of 5.5546 and 5.7941, respectively) of the antiplatelet target enzyme COX-1 depicting a strong binding affinity. However, the standard reference aspirin (IC_{50} = 21.59 ± 0.63; docking total score = 4.4422) showed slightly weaker interaction at Arg-120 binding site pocket residues of the COX-1 depicting a low binding affinity. Succinctly, this infer us that these class of 2-oxo-benzo[1,4]oxazines showed better antiplatelet activity due to greater binding affinity as compared to aspirin.

2.4 | Pharmacokinetic and toxicity study

These ADME descriptors were calculated for 2-oxo-2-phenyl-ethylidene linked 2-oxo-benzo[1,4]oxazine analogues and compared with standard ranges. All the analogues possessed a good number of hydrogen bond donors and acceptors.[26c,d] These derivatives were designed to increase the binding of the drug with the receptor through hydrogen bonding. These derivatives were found to follow Lipinski's rule of 5, affording drug likeness to the designed compounds. Polar surface area was calculated to estimate the ability of the compounds to permeate cell membranes. Lipophilicity was (ratio of octanol solubility to water solubility) measured through log P, which has been implicated in blood brain barrier penetration and permeability prediction. The excretion of drugs depends on molecular weight and log *P*-values.[26e–h] Succinctly, the

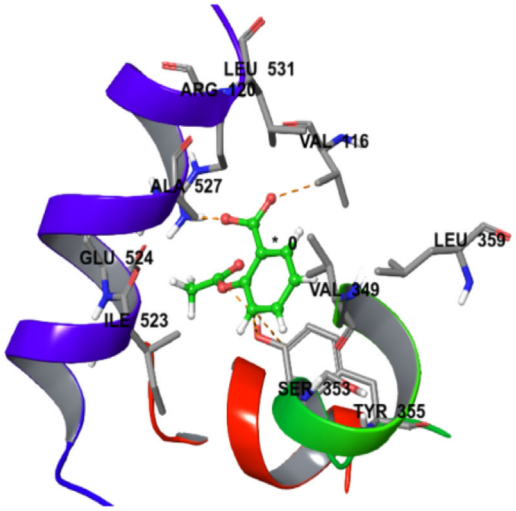

6

FIGURE 6 Predicted interactions of aspirin with antiplatelet target enzyme COX-1 (PDB: 2OYE) with a docking total score of 4.4422, revealing a H-bond of length 1.8, to the binding site pocket residues Arg-120

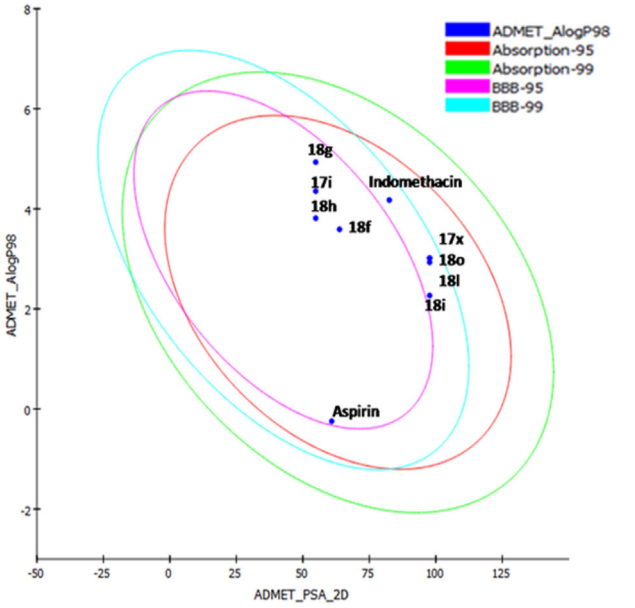

FIGURE 7 Plot of polar surface area (PSA) versus ALogP for 2-oxo-2-phenylethylidene linked 2-oxo-benzo[1,4]oxazine analogues **17i**, **17x**, **18f–i**, **18l**, and **18o**. The 95 and 99% confidence limit ellipses corresponding to the blood–brain barrier (BBB) and intestinal absorption are shown separately

2-oxo-2-phenylethylidene linked 2-oxo-benzo[1,4]oxazine analogues showed significant antiplatelet activity having some pharmacokinetic (PK) limitations.

The calculated TPSA (topological polar surface area) values of these compounds were within acceptable limits. The distribution of compounds in the human body was described by the predicted blood–brain barrier coefficient (logBB), apparent Caco-2 permeability, log Kp for skin permeability, volume of distribution and plasma protein binding (log Khsa for serum protein binding).[27f–h] All compounds show good aqueous solubility (Supporting Information Table S1). Functionalized antiplatelet active and promising analogues of 2-oxo-benzo[1,4]oxazines (i.e., **17i**, **17x**, **18f–18i**, **18l**, and **18o**) were also analyzed for permeability compliance, a key determinant factor in ADMET studies or prior to clinical trials, with the help of human skin and human jejunal effective permeability parameters, along with apparent Madin-Darby Canine Kidney Cells-On-Sheet (MDCK COS) permeability, and permeability through rabbit cornea as well as permeability through human skin. MDCK permeability was in acceptable limit. Moreover, ADMET results of predicted all analogues revealed liver high intrinsic passive uptake capacity, which is considered safe in sense of pharmacology studies. Also, calculated the brain/blood partition coefficient was detected (in logarithm), whereas the percent unbound to blood plasma proteins was detected under acceptable limit. The calculated values for these ADME parameters showed close similarity between the analogues and that of the reference drug aspirin and lie within the standard range of values exhibited by 95% of known drugs shown in Figure 7.

3 | CONCLUSION

We have successfully designed and synthesized a series of functionalized 2-oxo-phenylidene linked functionalized 2-oxo-benz-[1,4]oxazine analogues **17a–x** and **18a–o**, whose activities as platelet aggregation inhibitory activity as well as their SAR and cytotoxic studies followed by validation of results via *in silico* molecular docking simulation studies, were further investigated. Compounds **17a–x** and **18a–o** possessed moderate to good AA induced platelet aggregation inhibitory activities as compared to standard drug aspirin. Among all the tested compounds, three compounds (**17i**, **18g**, and **18h**) exhibited comparable platelet aggregation inhibition activity to aspirin, whereas five compounds (**17x**, **18f**, **18i**, **18l**, and **18o**) showed greater aggregation inhibitory activity than aspirin. The cytotoxicity of these compounds were found to be non-toxic in nature in 3T3 fibroblast cell line in MTT assay. Moreover, the *in silico* molecular docking simulation studies were also performed to validate the platelet aggregation inhibitory activity of active compounds. To the best of our knowledge, this is the first report of the identification, SAR and *in silico* molecular docking studies of 2-oxo-benz[1,4]oxazines as a novel AA-induced platelet aggregation inhibitors. These findings serve functionalized 2-oxo-benz[1,4]-oxazines as a promising scaffold to develop as hopeful inhibitors and aiming to improve the activity in order to get more potent and active platelet aggregation inhibitors. Further structural modifications are currently in progress in our laboratory and will be updated in other reports.

4 | EXPERIMENTAL

4.1 | Chemistry

4.1.1 | General

All glass apparatus were completely oven dried prior to use. Melting points were taken in open capillaries using complab melting point apparatus and are presented uncorrected. Ultrasonic irradiation was performed in a Elmasonic S 30 (H) ultrasonic water bath cleaner and the reaction vessel was positioned in the maximum energy area in the cleaner and the removal or addition of water was used to control the temperature of the water bath. Infrared spectra were recorded on a Perkin-Elmer FT-IR Spectrum 2 spectrophotometer. ^{1}H NMR and ^{13}C NMR spectra were recorded on ECS 400 MHz (JEOL) NMR spectrometer using $CDCl_3$, and CD_3SOCD_3 as well as mixture of ($CDCl_3$ + CD_3SOCD_3) as solvent and tetramethylsilane as internal reference. Electrospray ionization mass spectrometry (ESI-MS) and HRMS were recorded on Xevo G2-S Q-TOF (Waters, USA) spectrometer. Column chromatography was performed over Merck silica gel (particle size: 60–120 mesh) procured from Qualigens™ (India), flash silica gel (particle size: 230–400 mesh). All chemicals and reagents were obtained from Sigma–Aldrich (USA), Merck (India), or Spectrochem (India) and were used without further purification.

Copies of the ^{1}H and ^{13}C spectral data of the novel and active compounds, a table showing the pharmacokinetic and toxicity properties of the 2-oxo-benzo[1,4]oxazin-2-ones **17i**, **17x**, **18f–i**, **18l**, and **18o**, and statistical analysis calculations for the platelet aggregation inhibitory activity can be found in the Supporting Information. The InChI codes of the investigated compounds together with some biological activity data are also provided as Supporting Information.

4.1.2 | General procedure for the synthesis of the starting compounds, i.e., the substituted diketo-acids (15a–g)

Substituted acetophenones **12a–g** (1.00 mmol, 1 eq.) were taken in toluene (40 mL) and NaH (1.20 mmol, 1.2 eq.) was added cautiously. After stirring the reaction mixture at 0°C for 30 min, dimethyl oxalate **13** (1.00 mmol, 1 eq.) was added and heated at 80°C for 5–6 h (depending upon the substrate used). The progresses of the reaction were monitored by TLC using 9:1 hexane/ethyl acetate as an eluent. After completion of the reaction, the reaction mixture was quenched with distilled water (2 mL) and extracted with ethyl acetate (3 × 50 mL), washed with distilled water (50 mL), then with brine (3 × 20 mL). The combined organic layer was dried over anhyd. Na_2SO_4 and concentrated under reduced pressure. The resultant crude products were purified by recrystallization using EtOAc/hexane (v/v = 20:80), which afforded the pure desired diketo-esters **14a–g** in 72–94% yields. Compounds **14a–g** were used for next step without any further purification.

To a solution of **14a–g** (1.00 mmol, 1 eq.) in MeOH/THF/H_2O (15 mL, 7:2:1) was added LiOH.H_2O (1.30 mmol, 1.3 eq.) at 0°C, and stirred for 4–6 h at room temperature (depending upon the substrate used). The progresses of the reaction were monitored by TLC using hexane/ethyl acetate (30:70) as an eluent. After completion of the reaction, the reaction mixture was quenched by 3 N HCl and extracted with ethyl acetate (3 × 50 mL), washed with distilled water (50 mL), then with brine (3 × 20 mL). The combined organic layer was dried over anhyd. Na_2SO_4 and concentrated under reduced pressure. The resultant crude products were further purified by recrystallization using EtOAc/hexane (v/v = 10:90), which furnished the pure diketo-acids **15a–g** in good yields (86–97%). Compounds **15a–g** were used for next step without any further purification.

4.1.3 | General procedure for the synthesis of functionalized benzo[1,4]oxazin-2-ones (17a–x and 18a–o)

To a solution of the compounds **15a–g** (0.20 mmol; 1 eq.) in water (2.0 mL) was added compounds **16a–f** (0.20 mmol; 1 eq.) or **16e–g** (0.20 mmol; 1 eq.) and the reaction mixture was irradiated under ultrasonic sonicator at 80°C temperature for 75–120 min (depending upon the substrate employed). The progress of the reaction was monitored by TLC (9:1 hexane/ethyl acetate as an eluent). Then, the reaction mixture was extracted with ethyl acetate (3 × 10 mL), washed with distilled water (20 mL), then with brine (3 × 10 mL). The combined organic layer was dried over anhyd. Na_2SO_4 and concentrated under reduced pressure. The resultant crude products were further purified either by recrystallization using EtOAc/hexane (v/v = 10:90) or by flash column chromatography technique over silica gel (using 9:1 to 7:3 hexane/ethyl acetate as an eluent), which furnished the 2-oxo-benzo-[1,4]oxazine derivatives (**17a–x** and **18a–o**) in 78–98% yield range.

(*Z*)-3-(2-Oxo-2-phenylethylidene)-3,4-dihydro-2*H*-benzo[*b*]-[1,4]-oxazin-2-one (17a)

Yellowish solid; yield: 53.2 mg (98%), R_f (EtOAc/hexane; 20:80) = 0.85; m.p. 185–186°C; FT-IR (KBr, vmax/cm^{-1}) 3434, 1754, 1614, 1594, 1270, 1113; ^{1}H NMR (400 MHz, $CDCl_3$) δ 8.00 (d, *J* = 7.4 Hz, 2H), 7.56–7.47 (m, 3H), 7.21–7.06 (m, 5H); ^{13}C NMR (100 MHz, $CDCl_3$) δ 191.6, 156.3, 141.3, 139.1, 138.3, 132.8, 128.8, 127.7, 126.0, 124.0, 123.8, 117.2, 116.0, 94.7; HRMS (ESI) calcd. for $C_{16}H_{11}NO_3$ $[M+H]^+$: 266.0739. Found: 266.0744.

(*Z*)-6-Methyl-3-(2-oxo-2-phenylethylidene)-3,4-dihydro-2*H*-benzo[*b*][1,4]oxazin-2-one (17b)

Yellow solid; yield: 51.73 mg (93%), R_f (EtOAc/hexane; 20:80) = 0.90; m.p. 157–158°C; FT-IR (KBr, vmax/cm^{-1}) 3436, 1750, 1618, 1572, 1123, 740; ^{1}H NMR (400 MHz, $CDCl_3$) δ 8.00–7.98 (m, 2H), 7.56–7.45 (m, 3H), 7.07–7.02 (m, 2H), 6.88 (d, *J* = 8.5 Hz, 2H), 2.34 (s, 3H); ^{13}C NMR (100 MHz, $CDCl_3$) δ 191.5, 156.5, 139.4, 139.2, 138.4, 136.1, 132.7, 128.8, 127.7, 124.8, 123.4, 116.8, 116.2, 94.5, 21.08; HRMS (ESI) calcd. for $C_{17}H_{13}NO_3$ $[M+H]^+$: 280.0895. Found: 280.0899.

(*Z*)-6-Methyl-3-(2-oxo-2-(*p*-tolyl)ethylidene)-3,4-dihydro-2*H*-benzo[*b*][1,4]oxazin-2-one (17c)

Yellow solid; yield: 56.08 mg (96%), R_f (EtOAc/hexane; 20:80) = 0.80; m.p. 162–164°C; FT-IR (KBr, vmax/cm^{-1}) 3434, 1762, 1602, 1313, 1047; ^{1}H NMR (400 MHz, $CDCl_3$) δ 7.90 (d, *J* = 8.1 Hz, 2H), 7.27 (d, *J* = 8.0 Hz, 2H), 7.06 (d, *J* = 8.1 Hz, 1H), 7.02 (s, 1H), 6.88 (d, *J* = 9.4 Hz, 2H), 2.42 (s, 3H), 2.35 (s, 3H); ^{13}C NMR (100 MHz, $CDCl_3$) δ 191.3, 156.6, 143.5, 139.3, 139.0, 136.0, 135.8, 129.5, 127.8, 124.6, 123.5, 116.8, 116.1, 94.6, 21.7, 21.0; HRMS (ESI) calcd. for $C_{18}H_{15}NO_3$ $[M+H]^+$: 294.1052. Found: 294.1055.

(*Z*)-3-[2-(4-Methoxy-phenyl)-2-oxo-ethylidene]-6-methyl-3,4-dihydro-benzo[1,4]oxazin-2-one (17d)

Yellowish solid; yield: 57.7 mg (93%), R_f (EtOAc/hexane; 20:80) = 0.75; m.p. 180–182°C; FT-IR (KBr, vmax/cm^{-1}) 3452, 1755, 1625, 1581; ^{1}H NMR (400 MHz, $CDCl_3$) δ 7.99 (d, *J* = 8.8 Hz, 2H), 7.06 (d, *J* = 8.0 Hz, 1H), 7.00 (s, 1H), 6.96 (d, *J* = 9.4 Hz, 2H), 6.88–6.86 (m, 2H), 3.88 (s, 3H), 2.34 (s, 3H); ^{13}C NMR (100 MHz, $CDCl_3$) δ 190.4, 163.4, 156.8, 139.3, 138.7, 136.0, 131.3, 129.9, 124.4, 123.6, 116.8, 116.0, 114.0, 94.5, 55.6, 21.1; HRMS (ESI) calcd. for $C_{18}H_{15}NO_4$ $[M+H]^+$: 310.1001. Found: 310.1009.

(*Z*)-3-[2-(2,4-Dichloro-phenyl)-2-oxo-ethylidene]-6-methyl-3,4-dihydro-benzo[1,4]oxazin-2-one (17e)

Yellowish solid; yield: 65.4 mg (94%), R_f (EtOAc/hexane; 20:80) = 0.80; m.p. 142–145°C; FT-IR (KBr, vmax/cm^{-1}) 3436, 2913, 1755, 1618, 1570, 1083; ^{1}H NMR (400 MHz, $CDCl_3$) δ 7.53 (d, *J* = 8.3 Hz, 1H), 7.45 (d, *J* = 2.0 Hz, 1H), 7.33–7.30 (m, 1H), 7.10–7.08 (m, 1H), 6.94–6.92 (m, 2H), 6.73 (s, 1H), 2.36 (s, 3H); ^{13}C NMR (100 MHz, $CDCl_3$) δ 191.6, 155.9, 139.5, 139.2, 137.5, 137.2, 136.2, 132.5, 130.7, 130.6, 127.4, 125.4, 123.0, 117.0, 116.4, 98.0, 21.1; HRMS (ESI) calcd. for $C_{17}H_{11}Cl_2NO_3$ $[M+2]^+$: 349.0116. Found: 349.0112.

(*Z*)-3-(2-(4-Fluorophenyl)-2-oxoethylidene)-6-methyl-3,4-dihydro-2*H*-benzo[1,4]oxazin-2-one (17f)

Yellowish solid; yield: 53.7 mg (90%); R_f (EtOAc/hexane; 20:80) = 0.85; m.p. 145–147°C; FT-IR (KBr, vmax/cm^{-1}) 3433, 2930, 1770, 1624, 1596, 1128; ^{1}H NMR (400 MHz, $CDCl_3$) δ 8.02 (dd, *J* = 5.6, 8.8 Hz, 2H), 7.17–7.07 (m, 3H), 6.98–6.90 (m, 3H), 2.36 (s, 1H); ^{13}C NMR (100 MHz, $CDCl_3$) δ 190.0, 166.9, 156.4, 139.3, 136.1, 134.7, 130.3, 130.2, 124.9, 123.3, 116.9, 116.2, 115.9, 115.8, 94.1, 21.1; HRMS (ESI) calcd. for $C_{17}H_{12}FNO_3$ $[M+H]^+$: 298.0801. Found: 298.0807.

(*Z*)-3-(2-(4-Bromophenyl)-2-oxoethylidene)-6-methyl-3,4-dihydro-2*H*-benzo[*b*][1,4]oxazin-2-one (17g)

Yellow solid; yield: 66.48 mg (93%); R_f (EtOAc/hexane; 20:80) = 0.85; m.p. 179–181°C; FT-IR (KBr, vmax/cm^{-1}) 3435, 2923, 1763, 1624, 1543, 1052; ^{1}H NMR (400 MHz, $CDCl_3$) δ 7.87–7.84 (m, 2H), 7.63–7.59 (m, 2H), 7.08 (d, *J* = 9.2 Hz, 1H), 6.96 (s, 1H), 6.92–6.90 (m, 2H), 2.35 (s, 3H); ^{13}C NMR (100 MHz, $CDCl_3$) δ 190.2, 156.3, 139.5, 139.4, 137.1, 136.2, 132.0, 129.2, 127.7, 125.1, 123.2, 117.0, 116.3, 94.0, 21.1; HRMS (ESI) calcd. for $C_{17}H_{12}BrNO_3$ $[M+H]^+$: 358.0001. Found: 358.0007.

(*Z*)-8-Bromo-3-(2-(4-fluorophenyl)-2-oxoethylidene)-6-methyl-3,4-dihydro-2*H*-benzo[*b*][1,4]oxazin-2-one (17h)

Yellowish solid; yield: 67.6 mg (90%); R_f (EtOAc/hexane; 20:80) = 0.80; m.p. 230–232°C; FT-IR (KBr, vmax/cm^{-1}) 3417, 1771, 1631, 1285, 1159; ^{1}H NMR (400 MHz, $CDCl_3$) δ 8.03–7.99 (m, 2H), 7.17–7.13 (m, 3H), 6.99 (s, 1H), 6.84 (brs, 1H), 2.34 (s, 3H); ^{13}C NMR (100 MHz, $CDCl_3$) δ 190.1, 167.0, 164.5, 155.6, 138.7, 136.9, 136.6, 134.5, 134.4, 130.4, 130.3, 128.3, 124.6, 116.1, 115.9, 115.5, 110.2, 94.8, 20.9; HRMS (ESI) calcd. for $C_{17}H_{11}BrFNO_3$ $[M+2]^+$: 376.9906. Found: 376.9909.

(*Z*)-8-Bromo-3-(2-(4-bromophenyl)-2-oxoethylidene)-6-methyl-3,4-dihydro-2*H*-benzo[*b*][1,4]oxazin-2-one (17i)

Yellowish solid; yield: 77.6 mg (89%); R_f (EtOAc/hexane; 20:80) = 0.90; m.p. 259–260°C; FT-IR (KBr, vmax/cm^{-1}) 3417, 1768, 1629, 1562, 1283, 1138; ^{1}H NMR (400 MHz, $CDCl_3$) δ 7.86 (d, *J* = 8.8 Hz, 2H), 7.62 (d, *J* = 8.4 Hz, 2H), 7.16 (s, 1H), 7.00 (s, 1H), 6.86 (s, 1H), 2.35 (s, 3H); ^{13}C NMR (100 MHz, $CDCl_3$) δ 190.4, 155.6, 139.0, 137.0, 136.9, 136.7, 132.2, 129.3, 128.5, 128.1, 124.5, 115.6, 110.3, 94.8, 20.9; HRMS (ESI) calcd. for $C_{17}H_{11}Br_2NO_3$ $[M+2]^+$: 436.9106. Found: 436.9100.

(*Z*)-6-Chloro-3-(2-oxo-2-phenylethylidene)-3,4-dihydro-2*H*-benzo[*b*][1,4]oxazin-2-one (17j)

Yellowish solid; yield: 57.2 mg (95%), R_f (EtOAc/hexane; 20:80) = 0.80; m.p. 185–187°C; FT-IR (KBr, vmax/cm^{-1}) 3434, 1761, 1555, 1622, 1174; ^{1}H NMR (400 MHz, $CDCl_3$) δ 8.00–7.98 (m, 2H), 7.58–7.55 (m, 1H), 7.50–7.47 (m, 2H), 7.13–7.03 (m, 4H); ^{13}C NMR (100 MHz, $CDCl_3$) δ 191.8, 155.8, 139.8, 138.4, 138.1, 133.0, 131.1, 128.9, 127.8, 124.8, 123.8, 118.3, 115.8, 95.7; HRMS (ESI) calcd. for $C_{16}H_{10}ClNO_3$ $[M+2]^+$: 301.7085. Found: 301.7089.

(*Z*)-6-Chloro-3-(2-oxo-2-(*p*-tolyl)ethylidene)-3,4-dihydro-2*H*-benzo[*b*][1,4]oxazin-2-one (17k)

Yellowish solid; yield: 60.7 mg (95%); R_f (EtOAc/hexane; 20:80) = 0.90; m.p. 160–162°C; FT-IR (KBr, vmax/cm^{-1}) 3434, 2925, 1624, 1766, 1494, 1178; ^{1}H NMR (400 MHz, $CDCl_3$) δ 7.94–7.92 (m, 2H), 7.30 (d, *J* = 8.0 Hz, 2H), 7.14–7.04 (m, 4H), 2.44 (s, 3H); ^{13}C NMR (100 MHz, $CDCl_3$) δ 191.6, 156.0, 144.0, 139.8, 138.2, 135.6, 131.2, 129.7, 128.0, 125.0, 123.7, 118.3, 115.8, 95.9, 21.8; HRMS (ESI) calcd. for $C_{17}H_{12}ClNO_3$ $[M+H]^+$: 314.0506. Found: 314.0509.

(*Z*)-6-Chloro-3-(2-(4-chlorophenyl)-2-oxoethylidene)-3,4-dihydro-2*H*-benzo[*b*][1,4]oxazin-2-one (17l)

Yellowish solid; yield: 65.2 mg (95%); R_f (EtOAc/hexane; 20:80) = 0.90; m.p. 182–185°C; FT-IR (KBr, vmax/cm^{-1}) 3434, 1761, 1631, 1586, 1088; ^{1}H NMR (400 MHz, $CDCl_3$) δ 7.93 (d, *J* = 8.2 Hz, 2H), 7.45 (d, *J* = 8.1 Hz, 2H), 7.13–7.00 (m, 4H); ^{13}C NMR (100 MHz, $CDCl_3$) δ 190.4, 155.7, 139.8, 139.4, 138.7, 136.3, 131.2, 129.2, 129.1,

124.6, 124.0, 118.3, 115.9, 95.3; HRMS (ESI) calcd. for $C_{16}H_9Cl_2NO_3$ $[M+2]^+$: 334.9959. Found: 334.9956.

(*Z*)-6-Chloro-3-(2-(4-fluorophenyl)-2-oxoethylidene)-3,4-dihydro-2*H*-benzo[*b*][1,4]oxazin-2-one (17m)

Yellowish solid; yield: 57.8 mg (93%); R_f (EtOAc/hexane; 20:80) = 0.80; m.p. 155–157°C; FT-IR (KBr, vmax/cm^{-1}) 3434, 1754, 1634, 1601, 1495, 1226, 1160; ^{1}H NMR (400 MHz, $CDCl_3$) δ 8.06–8.02 (m, 2H), 7.20–7.13 (m, 4H), 7.08–7.04 (m, 2H); ^{13}C NMR (100 MHz, $CDCl_3$) δ 190.4, 155.8, 139.8, 138.6, 131.3, 130.5, 130.4, 124.8, 123.9, 118.4, 116.2, 115.9, 115.8, 95.4; HRMS (ESI) calcd. for $C_{16}H_9ClFNO_3$ $[M+H]^+$: 318.0255. Found: 318.0259.

(*Z*)-3-(2-(4-Bromophenyl)-2-oxoethylidene)-6-chloro-3,4-dihydro-2*H*-benzo[*b*][1,4]oxazin-2-one (17n)

Yellowish solid; yield: 71.5 mg (92%); R_f (EtOAc/hexane; 20:80) = 0.80; m.p. 175–177°C; FT-IR (KBr, vmax/cm^{-1}) 3436, 2924, 1755, 1632, 1583, 1007; ^{1}H NMR (400 MHz, $CDCl_3$) δ 7.85 (d, *J* = 7.9 Hz, 2H), 7.62 (d, *J* = 7.9 Hz, 2H), 7.13–7.00 (m, 4H); ^{13}C NMR (100 MHz, $CDCl_3$) δ 190.5, 155.6, 139.8, 138.8, 136.8, 132.1, 131.2, 129.3, 128.1, 124.6, 124.0, 118.3, 115.9, 95.2; HRMS (ESI) calcd. for $C_{16}H_9BrClNO_3$ $[M+2]^+$: 377.9454. Found: 377.9458.

(*Z*)-6-Chloro-3-(2-(4-methoxyphenyl)-2-oxoethylidene)-3,4-dihydro-2*H*-benzo[*b*][1,4]oxazin-2-one (17o)

Yellowish solid; yield: 62.6 mg (90%); R_f (EtOAc/hexane; 20:80) = 0.80; m.p. 178–180°C; FT-IR (KBr, vmax/cm^{-1}) 3434, 1764, 1628, 1594, 1018; ^{1}H NMR (400 MHz, $CDCl_3$) δ 7.99–7.97 (m, 2H), 7.10–7.06 (m, 2H), 7.02–6.99 (m, 2H), 6.97–6.94 (m, 2H), 3.87 (s, 3H); ^{13}C NMR (100 MHz, $CDCl_3$) δ 190.5, 163.7, 156.1, 139.6, 137.8, 131.1, 130.9, 130.1, 125.0, 123.4, 118.2, 115.6, 114.1, 95.7, 55.6; HRMS (ESI) calcd. for $C_{17}H_{12}ClNO_4$ $[M+2]^+$: 331.7345. Found: 331.7349.

(*Z*)-6-Nitro-3-(2-oxo-2-phenylethylidene)-3,4-dihydro-2*H*-benzo[*b*][1,4]oxazin-2-one (17p)

Yellowish solid; yield: 57.2 mg (89%); R_f (EtOAc/hexane; 20:80) = 0.85; m.p. 198–200°C; FT-IR (KBr, vmax/cm^{-1}) 3436, 2928, 1762, 1625, 1581, 1142; ^{1}H NMR (400 MHz, $CDCl_3$) δ 8.03–7.96 (m, 4H), 7.61–7.49 (m, 3H), 7.31 (d, *J* = 8.8 Hz, 1H), 7.15 (s, 1H); ^{13}C NMR (100 MHz, $CDCl_3$) δ 192.1, 155.1, 145.2, 144.9, 137.7, 137.6, 133.4, 128.9, 127.9, 124.7, 118.9, 118.0, 111.5, 96.9; HRMS (ESI) calcd. for $C_{16}H_{10}N_2O_5$ $[M+H]^+$: 311.0590. Found: 311.0593.

(*Z*)-6-Nitro-3-(2-oxo-2-(*p*-tolyl)ethylidene)-3,4-dihydro-2*H*-benzo[*b*][1,4]oxazin-2-one (17q)

Yellow solid; yield: 53.99 mg (83%); R_f (EtOAc/hexane; 20:80) = 0.75; m.p. 220–223°C; FT-IR (KBr, vmax/cm^{-1}) 3433, 1760, 1624, 1524, 1109; ^{1}H NMR (400 MHz, DMSO-d_6) δ 8.73 (d, *J* = 2.4 Hz, 1H), 7.96–7.92 (m, 3H), 7.46–7.37 (m, 3H), 6.95 (s, 1H), 2.40 (s, 3H); ^{13}C NMR (100 MHz, DMSO-d_6) 189.9, 155.7, 145.9, 143.8, 139.2, 138.5, 135.2, 130.1, 128.1, 119.5, 118.9, 117.7, 112.6, 94.8, 21.7; HRMS (ESI) calcd. for $C_{17}H_{12}N_2O_5$ $[M+H]^+$: 325.0746. Found: 325.0741.

(*Z*)-3-(2-(4-Methoxyphenyl)-2-oxoethylidene)-6-nitro-3,4-dihydro-2*H*-benzo[*b*][1,4]oxazin-2-one (17r)

Yellowish solid; yield: 60.4 mg (86%); R_f (EtOAc/hexane; 20:80) = 0.75; m.p. 195–197°C; FT-IR (KBr, vmax/cm^{-1}) 3435, 2926, 1599, 1758, 1633, 1594; ^{1}H NMR (400 MHz, $CDCl_3$) δ 8.02–7.93 (m, 4H), 7.29 (d, *J* = 8.9 Hz, 1H), 7.10 (s, 1H), 6.98 (d, *J* = 8.7 Hz, 2H), 3.89 (s, 3H); ^{13}C NMR (100 MHz, $CDCl_3$) δ 190.7, 164.0, 155.3, 145.2, 144.9, 137.0, 130.7, 130.3, 124.9, 118.6, 117.8, 114.2, 111.2, 97.0, 55.7; HRMS (ESI) calcd. for $C_{17}H_{12}N_2O_6$ $[M+H]^+$: 341.0695. Found: 341.0692.

(*Z*)-3-(2-(4-Chlorophenyl)-2-oxoethylidene)-6-nitro-3,4-dihydro-2*H*-benzo[*b*][1,4]oxazin-2-one (17s)

Yellow solid; yield: 55.88 mg (81%); R_f (EtOAc/hexane; 20:80) = 0.70; m.p. 239–240°C; FT-IR (KBr, vmax/cm^{-1}) 3435, 2924, 1622, 1525, 1272; ^{1}H NMR (400 MHz, DMSO-d_6) δ 8.73 (s, 1H), 8.03 (d, *J* = 7.2 Hz, 2H), 7.91 (d, *J* = 9.1 Hz), 7.59 (d, *J* = 7.2 Hz, 2H), 7.42 (d, *J* = 9.0 Hz, 1H), 6.90 (s, 1H); ^{13}C NMR (100 MHz, DMSO-d_6) δ 188.9, 156.0, 146.0, 144.7, 139.8, 138.2, 137.1, 129.9, 129.6, 125.8, 119.0, 117.8, 113.1, 94.4; HRMS (ESI) calcd. for $C_{16}H_9ClN_2O_5$ $[M+2H]^+$: 346.0200. Found: 346.0204.

(*Z*)-3-(2-(2,4-Dichlorophenyl)-2-oxoethylidene)-6-nitro-3,4-dihydro-2*H*-benzo[*b*][1,4]oxazin-2-one (17t)

Yellow solid; yield: 64.05 mg (84%), R_f (EtOAc/hexane; 20:80) = 0.75; m.p. 185–187°C; FT-IR (KBr, vmax/cm^{-1}) 3588, 2930, 1769, 1585, 1685, 1108; ^{1}H NMR (400 MHz, $CDCl_3$) δ 8.05–7.99 (m, 2H), 7.55 (d, J = 8.4 Hz, 1H), 7.48 (d, J = 2.0 Hz, 1H), 7.37–7.33 (m, 2H), 6.89 (s, 1H); ^{13}C NMR (100 MHz, $CDCl_3$) δ 192.4, 154.5, 145.2, 145.1, 138.0, 137.6, 136.9, 132.7, 131.0, 130.8, 127.6, 124.2, 119.4, 118.1, 111.7, 100.4; HRMS (ESI) calcd. for $C_{16}H_8Cl_2N_2O_5$ $[M+2H]^+$: 379.9810. Found: 379.9815.

(*Z*)-3-(2-(4-Fluorophenyl)-2-oxoethylidene)-6-nitro-3,4-dihydro-2*H*-benzo[*b*][1,4]oxazin-2-one (17u)

Yellowish solid; yield: 62.2 mg (94%); R_f (EtOAc/hexane; 20:80) = 0.75; m.p. >250°C; FT-IR (KBr, vmax/cm^{-1}) 3435, 3107, 1759, 1622, 1594, 1156; ^{1}H NMR (400 MHz, DMSO-d_6) δ 8.73 (s, 1H), 8.11 (d, *J* = 5.2 Hz, 2H), 7.92 (d, *J* = 6.4 Hz, 1H), 7.44–7.36 (m, 3H), 6.92 (s, 1H); ^{13}C NMR (100 MHz, DMSO-d_6) δ 188.7, 156.0, 145.9, 144.6, 139.5, 135.1, 130.9, 125.8, 118.9, 117.7, 116.6, 116.4, 113.0, 94.5; HRMS (ESI) calcd. for $C_{16}H_9FN_2O_5$ $[M+H]^+$: 329.0495. Found: 329.0490.

(*Z*)-3-(2-(4-Bromophenyl)-2-oxoethylidene)-6-nitro-3,4-dihydro-2*H*-benzo[*b*][1,4]oxazin-2-one (17v)

Yellow solid; yield: 60.92 mg (78%); R_f (EtOAc/hexane; 20:80) = 0.70; m.p. 195–197°C; FT-IR (KBr, vmax/cm^{-1}) 3435, 2925, 1759, 1525, 1023; ^{1}H NMR (400 MHz, $CDCl_3$) δ 8.03–7.97 (m, 2H), 7.89–7.86 (m, 2H), 7.66–7.63 (m, 2H), 7.32 (d, *J* = 9.2 Hz, 1H), 7.07 (s, 1H); ^{13}C NMR (100 MHz, $CDCl_3$) δ 190.8, 154.9, 145.3, 145.0, 138.0, 136.5, 132.3, 129.4, 128.6, 124.5, 119.2, 118.0, 111.6, 96.4; HRMS (ESI) calcd. for $C_{16}H_9BrN_2O_5$ $[M+2H]^+$: 389.9695. Found: 389.9699.

(*Z*)-7-Nitro-3-(2-oxo-2-phenylethylidene)-3,4-dihydro-2*H*-benzo[*b*][1,4]oxazin-2-one (17w)

Yellowish solid; yield: 57.5 mg (89%); R_f (EtOAc/hexane; 20:80) = 0.70; m.p. 240–242°C; FT-IR (KBr, vmax/cm^{-1}) 3436, 1763, 1622, 1596, 1268; ^{1}H NMR (400 MHz, $CDCl_3$) δ 8.06–8.00 (m, 4H), 7.83–7.81 (m, 1H), 7.62 (t, *J* = 7.3 Hz, 1H), 7.54 (t, *J* = 7.5 Hz, 2H), 6.99 (s, 1H); ^{13}C NMR (100 MHz, $CDCl_3$) 190.7, 156.1, 142.2, 141.1, 139.2, 138.3, 133.6, 131.3, 129.6, 128.0, 121.4, 117.4, 112.6, 96.0; HRMS (ESI) calcd. for $C_{16}H_{10}N_2O_5$ $[M+H]^+$: 311.0590. Found: 311.0595.

(*Z*)-3-(2-(4-Bromophenyl)-2-oxoethylidene)-7-nitro-3,4-dihydro-2*H*-benzo[*b*][1,4]oxazin-2-one (17x)

Yellowish solid; yield: 69.6 mg (87%); R_f (EtOAc/hexane; 20:80) = 0.80; m.p. 230–232°C; FT-IR (KBr, vmax/cm^{-1}) 3435, 3093, 1769, 1619, 1521; ^{1}H NMR (400 MHz, DMSO-d_6) δ 8.09–7.96 (m, 4H), 7.83–7.44 (m, 3H), 7.01 (d, *J* = 4.8 Hz, 1H); ^{13}C NMR (100 MHz, DMSO-d_6) δ 188.9, 154.7, 141.8, 140.1, 137.9, 136.6, 131.5, 130.0, 129.1, 126.6, 120.7, 116.5, 111.4, 95.7; HRMS (ESI) calcd. for $C_{16}H_9BrN_2O_5$ $[M+2]^+$: 389.9695. Found: 389.9691.

(*Z*)-3-(2-(4-Methoxyphenyl)-2-oxoethylidene)-7-nitro-3,4-dihydro-2*H*-benzo[*b*][1,4]oxazin-2-one (18a)

Yellowish solid; yield: 60.8 mg (92%); R_f (EtOAc/hexane; 20:80) = 0.70; m.p. 218–220°C; FT-IR (KBr, vmax/cm^{-1}) 3437, 2927, 2854, 1632, 1517; ^{1}H NMR (400 MHz, DMSO-d_6) δ 8.07–8.02 (m, 4H), 7.73 (d, *J* = 10.8 Hz, 1H), 7.09 (d, *J* = 8.8 Hz, 2H), 7.02 (s, 1H), 3.89 (s, 3H); ^{13}C NMR (100 MHz, DMSO-d_6) δ 189.1, 163.4, 155.8, 141.7, 140.6, 138.1, 131.1, 130.7, 130.1, 121.2, 116.8, 114.5, 112.2, 95.9, 55.8; HRMS (ESI) calcd. for $C_{17}H_{12}N_2O_6$ $[M+H]^+$: 341.0695. Found: 341.0699.

(*Z*)-3-(2-(4-Chlorophenyl)-2-oxoethylidene)-7-nitro-3,4-dihydro-2*H*-benzo[*b*][1,4]oxazin-2-one (18b)

Yellowish solid; yield: 63.2 mg (90%); R_f (EtOAc/hexane; 20:80) = 0.80; m.p. 205–207°C; FT-IR (KBr, vmax/cm^{-1}) 3432, 2925, 2860, 1633, 1525, 1776, 1075; ^{1}H NMR (400 MHz, DMSO-d_6) δ 8.08 (d, *J* = 8.4 Hz, 4H), 7.89–7.87 (m, 1H), 7.63 (d, *J* = 8.4 Hz, 2H), 7.01 (s, 1H); ^{13}C NMR (100 MHz, DMSO-d_6) δ 188.9, 155.4, 141.9, 140.7, 138.9, 136.5, 130.7, 129.8, 129.5, 129.2, 120.9, 117.0, 112.1, 95.2; HRMS (ESI) calcd. for $C_{16}H_9ClN_2O_5$ $[M+H]^+$: 345.0200. Found: 345.0207.

(*Z*)-3-(2-(2,4-Dichlorophenyl)-2-oxoethylidene)-7-nitro-3,4-dihydro-2*H*-benzo[*b*][1,4]oxazin-2-one (18c)

Yellowish solid; yield: 64.6 mg (85%); R_f (EtOAc/hexane; 20:80) = 0.70; m.p. 208–210°C; FT-IR (KBr, vmax/cm^{-1}) 3433, 3088, 1770, 1620, 1522, 1470, 1072; ^{1}H NMR (400 MHz, DMSO-d_6) δ 12.39 (s, 1H), 8.09–8.08 (m, 2H), 7.95–7.93 (s, 1H), 7.78–7.58 (m, 3H), 6.62 (s, 1H); ^{13}C NMR (100 MHz, DMSO-d_6) δ 190.3, 155.3, 142.2, 140.8, 138.5, 137.7, 136.2, 131.2, 131.0, 130.5, 130.1, 127.9, 120.8, 117.3, 112.1, 98.8; HRMS (ESI) calcd. for $C_{16}H_8Cl_2N_2O_5$ $[M+H]^+$: 378.9810. Found: 378.9818.

(*Z*)-3-(2-(4-Fluorophenyl)-2-oxoethylidene)-7-nitro-3,4-dihydro-2*H*-benzo[*b*][1,4]oxazin-2-one (18d)

Yellowish solid; yield: 52.7 mg (80%); R_f (EtOAc/hexane; 20:80) = 0.70; m.p. 235–237°C; FT-IR (KBr, vmax/cm^{-1}) 3411, 3090, 1773, 1626, 1516, 1473; ^{1}H NMR (400 MHz, DMSO-d_6) δ 8.18–8.08 (m, 4H), 7.88–7.86 (m, 1H), 7.42–7.38 (m, 2H), 7.02 (s, 1H); ^{13}C NMR (100 MHz, DMSO-d_6) 188.7, 163.7, 155.5, 141.8, 140.6, 138.7, 134.4, 130.7, 130.6, 130.5, 120.9, 116.9, 116.2, 115.9, 112.0, 95.3; HRMS (ESI) calcd. for $C_{16}H_9FN_2O_5$ $[M+H]^+$: 329.0495. Found: 329.0499.

(*Z*)-8-Bromo-6-methyl-3-(2-oxo-2-(*p*-tolyl)ethylidene)-3,4-dihydro-2*H*-benzo[*b*][1,4]oxazin-2-one (18e)

Yellowish solid; yield: 70.7 mg (95%); R_f (EtOAc/hexane; 20:80) = 0.90; m.p. 219–220°C; FT-IR (KBr, vmax/cm^{-1}) 3417, 1764, 1630, 1602, 1281, 1182; ^{1}H NMR (400 MHz, $CDCl_3$) δ 7.86 (d, 2H, *J* = 8.4 Hz, Ar-H), 7.24 (s, 1H, Ar-H), 7.08 (s, 1H, Ar-H), 7.00 (s, 1H, Ar-H), δ 6.80 (s, 1H, C═CH), 2.39 (s, 3H, CH_3), 2.30 (s, 3H); ^{13}C NMR (100 MHz, $CDCl_3$) δ 191.4, 155.8, 143.9, 138.3, 136.8, 136.5, 135.6, 129.6, 128.0, 127.9, 124.8, 115.4, 110.1, 95.3, 21.8, 20.9; HRMS (ESI) calcd. for $C_{18}H_{14}BrNO_3$ $[M+2]^+$: 373.0157. Found: 373.0152.

(*Z*)-8-Bromo-3-(2-(4-methoxyphenyl)-2-oxoethylidene)-6-methyl-3,4-dihydro-2*H*-benzo[*b*][1,4]oxazin-2-one (18f)

Yellowish solid; yield: 70.5 mg (91%); R_f (EtOAc/hexane; 20:80) = 0.80; m.p. 189–190°C; FT-IR (KBr, vmax/cm^{-1}) 3446, 2926, 1757, 1623, 1598, 1107; ^{1}H NMR (400 MHz, $CDCl_3$) δ 7.92 (d, *J* = 8.0 Hz, 2H), 7.03 (s, 1H), 6.90 (m, 3H), 6.74 (s, 1H), 3.84 (s, 3H), 2.28 (s, 3H); ^{13}C NMR (100 MHz, $CDCl_3$) δ 190.3, 163.5, 155.8, 137.9, 136.7, 136.4, 130.9, 130.0, 127.8, 124.8, 115.3, 114.0, 110.0, 95.1, 55.6, 20.9; HRMS (ESI) calcd. for $C_{18}H_{14}BrNO_4$ $[M+2]^+$: 389.0106. Found: 389.0109.

(*Z*)-8-Bromo-3-(2-(2,4-dichlorophenyl)-2-oxoethylidene)-6-methyl-3,4-dihydro-2*H*-benzo[*b*][1,4]oxazin-2-one (18g)

Yellowish solid; yield: 79.7 mg (94%); R_f (EtOAc/hexane; 20:80) = 0.85; m.p. 224–226°C; FT-IR (KBr, vmax/cm^{-1}) 3417, 1763, 1626, 1561, 1294, 1127; ^{1}H NMR (400 MHz, $CDCl_3$) δ 7.54 (d, *J* = 8.4 Hz, 1H), 7.47 (s, 1H), 7.33 (d, *J* = 8.0 Hz, 1H), 7.18 (s, 1H), 6.88 (s, 1H), 6.79 (s, 1H), 2.35 (s, 3H); ^{13}C NMR (100 MHz, $CDCl_3$) δ 191.9, 155.2, 138.7, 137.5, 137.3, 137.0, 136.8, 132.7, 130.8, 130.7, 128.8, 127.5, 124.3, 115.7, 110.3, 98.8, 20.9; HRMS (ESI) calcd. for $C_{17}H_{10}BrCl_2NO_3$ $[M+2]^+$: 426.9221. Found: 426.9227.

(*Z*)-8-Bromo-3-(2-(4-fluorophenyl)-2-oxoethylidene)-6-methyl-3,4-dihydro-2*H*-benzo[*b*][1,4]oxazin-2-one (18h)

Yellowish solid; yield: 67.6 mg (90%); R_f (EtOAc/hexane; 20:80) = 0.80; m.p. 230–232°C; FT-IR (KBr, vmax/cm^{-1}) 3417, 1771, 1631, 1285, 1159; ^{1}H NMR (400 MHz, $CDCl_3$) δ 8.03–7.99 (m, 2H), 7.17–7.13 (m, 3H), 6.99 (s, 1H), 6.84 (brs, 1H), 2.34 (s, 3H); ^{13}C NMR (100 MHz, $CDCl_3$) δ 190.1, 167.0, 164.5, 155.6, 138.7, 136.9, 136.6, 134.5, 134.4, 130.4, 130.3, 128.3, 124.6, 116.1, 115.9, 115.5, 110.2,

94.8, 20.9; HRMS (ESI) calcd. for $C_{17}H_{11}BrFNO_3$ $[M+2]^+$: 376.9906. Found: 376.9909.

(*Z*)-5-Nitro-3-(2-oxo-2-phenylethylidene)-3,4-dihydro-2*H*-benzo[*b*][1,4]oxazin-2-one (18i)

Yellowish solid; yield: 55.7 mg (88%); R_f (EtOAc/hexane; 20:80) = 0.80; m.p. 210–212°C; FT-IR (neat) 3054, 1766, 1622, 1584, 1461, 1041; ^{1}H NMR (400 MHz, DMSO-d_6) δ 8.16 (d, *J* = 8.8 Hz, 1H), 8.08 (d, *J* = 7.2 Hz, 2H), 7.59 (t, *J* = 7.6 Hz, 1H), 7.52–7.47 (m, 3H), 7.29 (s, 1H), 7.15 (t, *J* = 8.0 Hz, 1H); ^{13}C NMR (100 MHz, DMSO-d_6) δ 191.5, 155.1, 142.6, 137.9, 135.5, 134.0, 133.5, 128.9, 128.3, 123.0, 122.8, 122.6, 121.6, 99.7; HRMS (ESI) calcd. for $C_{16}H_{10}N_2O_5$ $[M+H]^+$: 311.0590. Found: 311.0596.

(*Z*)-5-Nitro-3-(2-oxo-2-(*p*-tolyl)ethylidene)-3,4-dihydro-2*H*-benzo[*b*][1,4]oxazin-2-one (18j)

Brownish solid; yield: 51.5 mg (79%); R_f (EtOAc/hexane; 20:80) = 0.70; m.p. 230–232°C; FT-IR (KBr, vmax/cm^{-1}) 3442, 2925, 1771, 1629, 1525, 1178; ^{1}H NMR (400 MHz, DMSO-d_6) δ 8.13 (d, *J* = 8.0 Hz, 1H), 7.99 (d, *J* = 8.0 Hz, 2H), 7.67 (t, *J* = 8.4 Hz, 1H), 7.37 (d, *J* = 8.0 Hz, 2H), 7.27 (t, *J* = 8.8 Hz, 1H), 7.10 (s, 1H), 2.39 (s, 3H); ^{13}C NMR (100 MHz, DMSO-d_6) δ 189.9, 154.3, 143.2, 142.4, 136.5, 134.9, 133.2, 129.1, 127.3, 126.2, 122.3, 122.0, 121.3, 97.06, 96.9, 20.6; HRMS (ESI) calcd. for $C_{17}H_{12}N_2O_5$ $[M+H]^+$: 325.0746. Found: 325.0742.

(*Z*)-3-(2-(4-Methoxyphenyl)-2-oxoethylidene)-5-nitro-3,4-dihydro-2*H*-benzo[*b*][1,4]oxazin-2-one (18k)

Yellowish solid; yield: 55.3 mg (83%); R_f (EtOAc/hexane; 20:80) = 0.65; m.p. 244–246°C; FT-IR (KBr, vmax/cm^{-1}) 3417, 1764, 1631, 1598, 1524, 1257, 1168, 1319; ^{1}H NMR (400 MHz, DMSO-d_6) δ 8.14–8.08 (m, 3H), 7.68 (d, *J* = 8.0 Hz, 1H), 7.25 (t, *J* = 8.4 Hz, 1H), 7.10–7.08 (m, 3H), 3.87 (s, 3H); ^{13}C NMR (100 MHz, DMSO-d_6) δ 188.8, 163.1, 154.4, 142.3, 136.1, 133.1, 130.3, 129.6, 122.2, 121.1, 114.0, 113.8, 97.2, 96.9, 55.2; HRMS (ESI) calcd. for $C_{17}H_{12}N_2O_6$ $[M+H]^+$: 341.0695. Found: 341.0692.

(*Z*)-3-(2-(4-Chlorophenyl)-2-oxoethylidene)-5-nitro-3,4-dihydro-2*H*-benzo[*b*][1,4]oxazin-2-one (18l)

Yellowish solid; yield: 59.4 mg (86%); R_f (EtOAc/hexane; 20:80) = 0.75; m.p. 255–257°C; FT-IR (KBr, vmax/cm^{-1}) 3416, 1767, 1629, 1588, 1316, 1258, 1092; ^{1}H NMR (400 MHz, DMSO-d_6) δ 8.17–8.06 (m, 3H), 7.64–7.53 (m, 3H), 7.25 (t, *J* = 8.4 Hz, 1H), 7.10 (s, 1H); ^{13}C NMR (100 MHz, DMSO-d_6) δ 188.9, 153.9, 142.2, 138.1, 136.3, 135.9, 133.3, 128.8, 128.3, 122.1, 121.6, 121.4, 121.1, 97.2; HRMS (ESI) calcd. for $C_{16}H_9ClN_2O_5$ $[M+2]^+$: 346.0200. Found: 346.0204.

(*Z*)-3-(2-(2,4-Dichlorophenyl)-2-oxoethylidene)-5-nitro-3,4-dihydro-2*H*-benzo[*b*][1,4]oxazin-2-one (18m)

Yellowish solid; yield: 61.7 mg (81%); R_f (EtOAc/hexane; 20:80) = 0.75; m.p. 252–254°C; FT-IR (KBr, vmax/cm^{-1}) 3417, 1762, 1630, 1518, 1384, 1285, 1116; ^{1}H NMR (400 MHz, DMSO-d_6) δ 8.18–8.14 (m, 1H), 7.69–7.64 (m, 3H), 7.50 (d, *J* = 7.6 Hz, 1H), 7.29 (t, *J* = 8.4 Hz, 1H), 6.78 (s, 1H); ^{13}C NMR (100 MHz, DMSO-d_6) δ 190.3, 153.7, 142.4, 136.9, 136.2, 133.4, 131.1, 130.4, 129.5, 129.4, 127.2, 127.1, 122.3, 121.7, 121.4, 100.4; HRMS (ESI) calcd. for $C_{16}H_8Cl_2N_2O_5$ $[M+2]^+$: 379.9810. Found: 379.9815.

(*Z*)-3-(2-(4-Fluorophenyl)-2-oxoethylidene)-5-nitro-3,4-dihydro-2*H*-benzo[*b*][1,4]oxazin-2-one (18n)

Yellowish solid; yield: 58.6 mg (89%); R_f (EtOAc/hexane; 20:80) = 0.75; m.p. 269–271°C; FT-IR (KBr, vmax/cm^{-1}) 3417, 1760, 1628, 1595, 1514, 1279, 1256, 1237, 1159; ^{1}H NMR (400 MHz, DMSO-d_6) δ 8.21–8.14 (m, 3H), 7.71 (d, *J* = 7.6 Hz, 1H), 7.41–7.37 (m, 2H), 7.31–7.27 (m, 1H), 7.11 (s, 1H); ^{13}C NMR (100 MHz, DMSO-d_6) δ 189.8, 166.9, 164.4, 155.2, 143.4, 137.8, 135.1, 134.2, 131.2, 131.1, 123.4, 122.8, 122.3, 116.5, 97.73, 97.60; HRMS (ESI) calcd. for $C_{16}H_9FN_2O_5$ $[M+H]^+$: 329.0495. Found: 329.0498.

(*Z*)-3-(2-(4-Bromophenyl)-2-oxoethylidene)-5-nitro-3,4-dihydro-2*H*-benzo[*b*][1,4]oxazin-2-one (18o)

Yellowish solid; yield: 64.1 mg (82%); R_f (EtOAc/hexane; 20:80) = 0.75; m.p. 232–234°C; FT-IR (KBr, vmax/cm^{-1}) 3442, 3098, 1766, 1620, 1583, 1067; ^{1}H NMR (400 MHz, DMSO-d_6) δ 8.13 (d, *J* = 8.4 Hz, 1H), 7.99 (d, *J* = 7.6 Hz, 2H), 7.74 (d, *J* = 8.0 Hz, 2H), 7.65 (d, *J* = 8.0 Hz, 1H), 7.29 (t, *J* = 8.4 Hz, 1H), 7.09 (s, 1H); ^{13}C NMR (100 MHz, DMSO-d_6) δ 189.1, 154.1, 142.5, 137.1, 136.4, 133.3, 131.5, 129.2, 126.7, 122.4, 121.8, 121.5, 121.4, 96.4; HRMS (ESI) calcd. for $C_{16}H_9BrN_2O_5$ $[M+2]^+$: 389.9695. Found: 389.9699.

4.2 | Biological activity assays

4.2.1 | Platelet aggregation inhibitory activity evaluation

All synthesized 2-oxo-2-phenylethylidene linked 2-oxo-benzo[1,4]-oxazine analogues (**17a–x** and **18a–o)** were dissolved in DMSO before testing. In order to eliminate the effects of the solvent on aggregation, the final concentration of DMSO was fixed at 0.5%. Arachidonic acid (AA), EDTA (disodium salt), bovine serum albumin, and dimethyl sulfoxide (DMSO) were purchased from Sigma Chemical Co.

Blood was collected from the rabbit marginal ear vein (several studies established that rabbit platelets are surrogate to human platelets both *in vitro* as well as *in vivo*)[25] and was mixed with EDTA to a final concentration of 6 mM. It was centrifuged for 10 min at 90 g at room temperature, and the supernatant was obtained as platelet-rich plasma. The latter was further centrifuged at 500×*g* for 10 min. The platelet pellets were washed with Tyrode's solution (Ca^{+2}-free) containing 2 mM EDTA, 0.1 and 3.5 mg/mL bovine serum albumin, and centrifuged at 500×*g* for 10 min. Then, the pellets were washed with Tyrode's solution without EDTA. After centrifugation under the same conditions, the platelet pellets were finally suspended in Tyrode's solution of the following composition (mM): NaCl (136.8), KCl (2.8), $NaHCO_3$ (11.9), $MgCl_2$ (2.1), NaH_2-PO_4 (0.33), $CaCl_2$ (1.0), and glucose (11.2) containing bovine serum albumin (0.35%).

Aggregation was measured by a turbidimetric method using a Lumi-aggregometer (Chrono-Log Corp., Havertown, PA). All glassware was siliconized. Three minutes before the addition of the aggregation inducer, the platelet suspension was stirred at 1200 rpm. The percentage of aggregation was calculated as follows (abs. = absorbance):

$$\%\text{Aggregation} = \frac{\text{Abs. of platelet suspension} - \text{Final abs. after aggregation}}{\text{Abs. of platelet suspension} - \text{abs. of Tyrode solution}} \times 100$$

Percent aggregation was expressed assuming the absorbance of platelet suspension as 0% aggregation and the absorbance of platelet-free Tyrode's solution as 100% aggregation. For each compound IC_{50} values were calculated by SigmaPlot.

4.2.2 | Cytotoxicity MTT assay[26]

The cytotoxic effect of the **17i**, **17x**, **18f**–**18i**, **18l**, and **18o** on cells were detected *in vitro* using the mitochondrial cytotoxic test. Cell viability was evaluated using thiazolyl blue tetrazolium bromide (MTT), which indicates the metabolic activity of cells. The experiment was performed in 96-well microplates. The cells were seeded at a density of 3.5×10^3 3T3 fibroblast cells per well. Samples were dissolved in DMSO (stock solution 10 mM) and subsequently diluted in medium to the final concentration of 25–250 μM (concentration of DMSO 0.5%) and after 24 h they were added to the cells. Microplates were cultivated for 72 h in thermostat at 37°C and 5% CO_2 atmosphere. After incubation thiazolyl blue tetrazolium bromide (3.33 mg/mL phosphate buffered saline, pH = 7.4) was pipetted to each well and left to incubate for further 2 h. Then the medium with MTT solution was removed. Formazan crystals in viable cells were dissolved in the lysis solution (4 mM HCl and 0.1% Nonidet P40 in ethanol). Microplates were shaken 15 min at 1500 rpm. Absorbance was measured at 540 nm and reference wavelength at 740 nm. Experiments were performed in triplicates and percent viability was calculated by dividing the OD obtained in treatment group by OD of the untreated cell control multiplied by hundred. Inhibition activity was expressed as percentages of control with DMSO.

4.3 | *In silico* molecular docking simulation studies

Molecular docking studies were performed via constructing 3D model of the structures using Surflex-Dock module in Sybyl-X 2.1 (Tripos International). The X-ray crystallographic structure of the ACC (PDB ID: 2OYE)[27a] solved at 2.85 Å resolution was retrieved from the PDB, and modified for docking calculations. Co-crystallized ligand indomethacin was removed from the binding site, water molecules were removed, —H atoms were added, and side chains were fixed during protein preparation. Protein structure minimization was performed by applying Tripos force field, and partial atomic charges were calculated by Gasteiger-Huckel method.[27b–d]

4.3.1 | Molecular docking

Molecular modeling studies of 2-oxo-2-phenylethylidene linked 2-oxo-benzo[1,4]oxazine analogues **17i**, **17x**, **18f**–**i**, **18l**, and **18o** were carried out using the molecular modeling software Sybyl-X 2.1 (Tripos International). Drawing of structures and simple geometry optimization were performed with ChemBio-Office suite Ultra v12.0 (2012) (Cambridge Soft Corp). The binding affinity of all compounds were predicted with the platelet aggregation inhibitor target enzyme cyclooxygenase-1 (COX-1). Energy minimization was done using the Tripos force field with a distance-dependent dielectric and the Powell gradient minimization algorithm, with a convergence criterion of 0.001 kcal/mol for the determination of conformations with the most favorable (lowest energy). Aromatase at 3.5 Å resolution (PDB: 2OYE)[27a] was selected. The crystal structure of COX-1 enzyme of sheep (it has been well established that COX-1 of sheep is almost similar to that of COX-1 of human)[27b,c] in complex with indomethacin obtained from the PDB. Hydrogen atoms were added to the protein with the protonation 3D tool in Sybyl. Partial atomic charges were assigned using the Gasteiger-Hückel method in Sybyl. All 2D structures were converted to 3D structures using the program Concord v4.0 and the maximum number of iterations performed in the energy minimization was set to 2000. Further geometry optimization was done with the MOPAC-6 package using the semi-empirical PM3 Hamiltonian method.[27d–g]

4.3.2 | Prediction of *in silico* pharmacokinetic and toxicity parameters

Pharmacokinetic (PK) properties depend on the chemical properties of drugs, which determine their absorption, distribution, metabolism, excretion, and toxicity (ADMET) properties, which are the key descriptors for the human therapeutic use of any compound. Predictive ADMET mathematical models were derived with different PK parameters, namely, aqueous solubility, blood–brain barrier penetration, cytochrome P-450 2D6 inhibition, hepatotoxicity, human intestinal absorption, and plasma protein binding. Predictions from these models were contrasted with known rules for appropriate ADMET characteristics for 2-oxo-2-phenylethylidene linked 2-oxo-benzo[1,4]oxazine analogues **17i**, **17x**, **18f**–**i**, **18l**, and **18o**. Some properties correlate well with PK, e.g, primary determinant of fractional absorption can be represented by polar surface area (PSA) (cut-off ≤140 $Å^2$) and low molecular weight (MW) for absorption.[27h–j] For secondary determination of fractional absorption (passive membrane transport), the sum of H-bond donors and acceptors (cut-off ≤12) was used. The number of rotatable bonds were used as a measure of flexibility (cut-off ≤10) and bioavailability. Drug distribution depends on a number of factors, such as permeability (indicated by apparent Caco-2 and MDCK permeability, log Kp for skin permeability), blood-brain barrier (log BB), the volume of distribution and plasma protein binding (log Khsa for serum protein binding).[27d–h] These ADME descriptors were calculated and compared with standard ranges. The octanol-water partition coefficient (logP) has been

implicated in BB penetration and permeability studies. The excretion of drugs from the body depends on logP and MW. Likewise, rapid renal clearance is associated with hydrophilicity and small MW. In the liver, drug metabolism is associated with hydrophobicity and large MW. Higher lipophilicity leads to poor absorption and increase in metabolic processes. ADME descriptors for 90% of orally active compounds follow Lipinski's rule of 5. These ADME parameters were calculated through Qikprop v3.2 (Schrödinger, LLC, USA, 2015 and Discovery Studio 3.5). The recommended toxicity screening models for carcinogenicity are developmental toxicity, mutagenicity, and skin irritancy or sensitization, and these were calculated with the DSTOPKAT module. These predictions are useful for the optimization of therapeutic ratios of lead compounds and assessment of their potential safety. These predictions also help in evaluating intermediates, metabolites and pollutants, along with setting dose range for animal assays.

ACKNOWLEDGMENTS

S.C. acknowledges SERB, New Delhi for Fast Track Scheme for young scientist (Grant no. CS-037/2013); DST, New Delhi for DST-RFBR Indo-Russian Joint Research Project (INT/RUS/RFBR/P-169); and CSIR, New Delhi for CSIR-EMR Grant [02(0189)/14/EMR-II]. V.S. thanks MNIT, Jaipur for providing financial assistance in the form of fellowship. P.K.J acknowledges CSIR, New Delhi for providing RA fellowship. D.K.Y acknowledges the National Research Foundation of Korea (NRF), which is funded by the Ministry of Education, Science, and Technology (No.: 2017R1C1B2003380) at the Gachon University, Incheon City, Korea. Materials Research Centre (MRC), MNIT, Jaipur is gratefully acknowledged for providing analytical facilities.

CONFLICT OF INTEREST

The authors declare no conflict of interest.

ORCID

Sandeep Chaudhary http://orcid.org/0000-0002-1444-3895

REFERENCES

[1] A. D. Lopez, C. D. Mathers, M. Ezzati, D. T. Jamison, C. J. Murray, *Lancet* **2006**, *367*, 1747.
[2] a) E. Falk, *Circulation* **1985**, *71*, 699; b) B. S. Coller, *N. Engl. J. Med.* **1990**, *322*, 33.
[3] B. S. Coller, *Circulation* **1995**, *92*, 2373.
[4] E. Van De Graaff, S. R. Steinhubl, *Ann. Med.* **2000**, *32*, 561.
[5] a) A. Schwienhorst, *Cell. Mol. Life Sci.* **2006**, *63*, 2773; b) S. Srivastava, L. N. Goswami, D. K. Dikshit, *Med. Res. Rev.* **2005**, *25*, 66.
[6] H. U. Stilz, B. Jablonka, M. Just, J. Knolle, E. F. Paulus, G. Zoller, *J. Med. Chem.* **1996**, *39*(11), 2118.
[7] W. F. Urmey, J. Rowlingson, *Reg. Anesth. Pain Med.* **1998**, *23*, 146.
[8] S. A. Andronati, T. L. Karaseva, A. A. Krysko, *Curr. Med. Chem.* **2004**, *11*, 1183.
[9] K. Jurk, B. E. Kehrel, *Semin. Thromb. Hemost.* **2005**, *31*, 381.
[10] a) K. Sangkuhl, A. R. Shuldiner, T. E. Klein, R. B. Altman, *Pharmacogenet. Genom.* **2011**, *21*, 516; b) J. M. Stassen, J. Arnout, H. Deckmyn, *Curr. Med. Chem.* **2004**, *11*, 2245; c) C. Patrono, *N. Engl. J. Med.* **1994**, *330*, 1287.
[11] a) O. Yasuda, Y. Takemura, H. Kawamoto, H. Rakugi, *Cell. Mol. Life Sci.* **2008**, *65*, 354; b) D. R. Phillips, I. F. Charo, L. V. Parise, L. A. Fitzgerald, *Blood* **1988**, *71*, 831.
[12] a) J. A. Zablocki, M. Miyano, R. B. Garland, D. Pireh, L. Schretzman, S. N. Rao, R. J. Lindmark, M. V. Toth, M. E. Zupec, D. E. McMackins, S. P. Adams, M. Miyano, C. S. Markos, M. N. Milton, S. Paulson, M. Herin, P. Jacqmin, N. S. Nicholson, S. G. Panzer-Knodle, N. F. Haas, J. D. Page, J. A. Szalony, B. B. Taite, A. K. Salyers, L. W. King, J. G. Campion, L. P. Feigen, *J. Med. Chem.* **1993**, *36*, 1811; b) D. F. Kong, R. M. Califf, D. P. Miller, D. J. Moliterno, H. D. White, R. A. Harrington, J. E. Tcheng, A. M. Lincoff, V. Hasselblad, E. J. Topol, *Circulation* **1998**, *98*, 2829.
[13] a) J. R. Leclerc, *Crit. Care Med.* **2002**, *30*, S332; b) M. J. Quinn, T. V. Byzova, J. Qin, E. J. Topol, E. F. Plow, *Arterioscler. Thromb. Vasc. Biol.* **2003**, *23*, 945.
[14] a) J. Ruef, H. A. Katus, *Expert Opin. Investig. Drugs* **2003**, *12*, 781; b) A. J. Lopez Farre, J. Tamargo, P. J. Mateos-Caceres, L. Azcona, C. Macaya, *Pharma. Res.* **2010**, *27*, 2365.
[15] a) B. C. Das, A. V. Madhukumar, J. Anguiano, S. Mani, *Bioorg. Med. Chem. Lett.* **2009**, *19*, 4204; b) H. Otsuka, Y. Hirai, T. Nagao, K. Yamasaki, *J. Nat. Prod.* **1988**, *51*, 74; c) B. P. Mathew, A. Kumar, S. Sharma, P. K. Shukla, M. Nath, *Eur. J. Med. Chem.* **2010**, *45*, 1502; d) H. B. Borate, S. R. Maujan, S. P. Sawargave, M. A. Chandavarkar, S. R. Vaiude, V. A. Joshi, R. D. Wakharkar, R. Iyer, R. G. Kelkar, S. P. Chavan, S. S. Kunte, *Bioorg. Med. Chem. Lett.* **2010**, *20*, 722; e) G. J. Reddy, S. Sailaja, K. S. Rao, P. Reddanna, D. B. Reddy, *Indian J. Chem., Sect. B: Org. Chem. Incl. Med. Chem.* **2005**, *44B*, 204; f) N. A. Powell, F. L. Ciske, C. Cai, D. D. Holsworth, K. Mennen, C. A. Van Huis, M. Jalaie, J. Day, M. Mastronardi, P. McConnell, I. Mochalkin, E. Zhang, M. J. Ryan, J. Bryant, W. Collard, S. Ferreira, C. Gu, R. Collins, J. J. Edmunds, *Bioorg. Med. Chem.* **2007**, *15*, 5912; g) P. Zhang, E. A. Terefenko, A. Fensome, Z. Zhang, Y. Zhu, J. Cohen, R. Winneker, J. Wrobel, J. Yardley, *Bioorg. Med. Chem. Lett.* **2002**, *12*, 787.
[16] a) X. Tian, L.-Y. Wang, S. Xia, Z.-B. Li, X.-H. Liu, Y. Yuan, L. Fang, H. Zuo, *Bioorg. Med. Chem. Lett.* **2012**, *22*, 204; b) S. Xia, J-Q. Liu, X-H. Wang, Y. Tian, Y. Wang, J-H. Wang, L. Fang, H. Zuo, *Bioorg. Med. Chem. Lett.* **2014**, *24*, 1479.
[17] D. A. Dudley, A. M. Bunker, L. G. Chi, W. L. Cody, D. R. Holland, D. P. Ignasiak, N. Janiczek-Dolphin, T. B. McClanahan, T. E. Mertz, L. S. Narasimhan, S. T. Rapundalo, J. A. Trautschold, C. A. Van Huis, J. J. Edmunds, *J. Med. Chem.* **2000**, *43*, 4063.
[18] a) P. Jakobsen, A. M. Horneman, E. Persson, *Bioorg. Med. Chem.* **2000**, *8*, 2803; b) P. Jakobsen, B. R. Pedersen, E. Persson, *Bioorg. Med. Chem.* **2000**, *8*, 2095.
[19] M. Anderluh, J. Cesar, P. Stefanic, D. Kikelj, D. Janes, J. Murn, K. Nadrah, M. Tominc, E. Addicks, A. Giannis, M. Stegnar, M. S. Dolenc, *Eur. J. Med. Chem.* **2005**, *40*, 25.
[20] J. Ilaš, Ž. Jakopin, T. Borštnar, M. Stegnar, D. Kikelj, *J. Med. Chem.* **2008**, *51*, 5617.
[21] P. Š. Anderluh, M. Anderluh, J. Ilaš, J. Mravljak, M. S. Dolenc, M. Stegnar, D. Kikelj, *J. Med. Chem.* **2005**, *48*, 3110.
[22] a) S. K. Ihmaid, J. M. A. Al-Rawi, C. J. Bradley, M. J. Angove, M. N. Robertson, *Eur. J. Med. Chem.* **2012**, *57*, 85; b) S. K. Ihmaid, J. M. A. Al-Rawi, C. J. Bradley, *Eur. J. Med. Chem.* **2010**, *45*, 4934; c) S. K. Ihmaid, J. M. A. Al-Rawi, C. J. Bradley, M. J. Angove, M. N. Robertson, R. L. Clark, *Bioorg. Med. Chem.* **2011**, *19*, 3983; d) K. M. Pritchard, J. M. A. Al-Rawi, C. J. Bradley, *Eur. J. Med. Chem.* **2007**, *42*, 1200; e) G. Roma, M. D. Braccio, G. Grossi, D. Piras, G. Leoncini, D. Bruzzese, M. G. Signorello, P. Fossa, L. Mosti, *J. Med. Chem.* **2007**, *50*, 2886; f) T.-C. Ko, M.-J. Hour, J.-C. Lien, C.-M. Teng, K.-H. Lee, S.-C. Kuo, L.-J.

Huang, *Bioorg. Med. Chem. Lett*. **2001**, *11*, 279; g) C. Kontogiorgis, O. Nicolotti, G. F. Mangiatordi, M. Tognolini, F. Karalaki, C. Giorgio, A. Patsilinakos, A. Carotti, D. Hadjipavlou-Litina, E. Barocelli, *J. Enzyme Inhib. Med. Chem*. **2015**, *30*(6), 925.

[23] a) P. K. Jaiswal, V. Sharma, J. Prikhodko, I. V. Mashevskaya, S. Chaudhary, *Tetrahedron Lett*. **2017**, *58*(22), 2077; b) R. Sharma, L. Yadav, J. Lal, P. K. Jaiswal, M. Mathur, A. K. Swami, S. Chaudhary, *Bioorg. Med. Chem. Lett*. **2017**, *27*(18), 4393.

[24] a) I. V. Mashevskaya, I. A. Tolmacheva, E. V. Voronova, T. F. Odegova, G. A. Aleksandrova, A. F. Goleneva, S. V. Kol'tsova, A. N. Maslivets, *Pharm. Chem. J*. **2002**, *36*(2), 33; b) Y. Iwanami, T. Seki, T. Inagaki, *Bull. Chem. Soc. Jpn*. **1971**, *44*(5), 1316; c) V. L. Gein, N. A. Rassudikhina, N. V. Shepelina, M. I. Vakhrin, E. B. Babushkina, E. V. Voronina, *Pharm. Chem. J*. **2008**, *42*(9), 529; d) M. Xia, B. Wu, G. Xiang, *J. Fluor. Chem*. **2008**, *129*(5), 402; e) E. E. Stepanova, Z. G. Aliev, A. N. Maslivets, *Russ. J. Org. Chem*. **2013**, *49*, 1762 and references cited therein.

[25] M. A. Packham, M. L. Rand, R. L. Kinlough-Rathbone, *Camp. Biochem. Physiol*. **1992**, *103A* (I), 35.

[26] M. Danihelová, M. Veverka, E. Šturdík, S. Jantová, *Interdiscip. Toxicol*. **2013**, *6*, 209.

[27] a) A. L. Lourenço, M. S. Saito, L. E. Dorneles, G. M. Viana, P. C. Sathler, L. C. Aguiar, M. de Pádula, T. F. Domingos, A. G. Fraga, C. R. Rodrigues, V. P. de Sousa, H. C. Castro, L. M. Cabral, *Molecules* **2015**, *20*, 7174; b) J. K. Gierse, J. J. McDonald, S. D. Hauser, S. H. Rangwala, C. M. Koboldt, K. Seibert, *J Biol. Chem*. **1996**, *271*(26), 15810; c) R. G. Huff, E. Bayram, H. Tan, S. T. Knutson, M. H. Knaggs, A. B. Richon, P. Santago, II, *Chem. Biodivers*. **2005**, *2*, 1533; d) D. K. Yadav, I. Ahmad, A. Shukla, F. Khan, A. S. Negi, A. Gupta, *J. Chemometrics* **2014**, *28*, 499; e) D. K. Yadav, F. Khan, *J. Chemometrics* **2013**, *27*, 21; f) D. K. Yadav, R. Rai, N. Kumar, S. Singh, S. Misra, P. Sharma., P. Shaw, H. Pérez-Sánchez, R. L. Mancera, E. H. Choi, M. H. Kim, R. Pratap, *Sci. Rep*. **2016**, *6*, 38128; g) D. K. Yadav, S. Dhawan, A. Chauhan, T. Qidwai, P. Sharma, R. S. Bhakuni, O. P. Dhawan, F. Khan, *Curr. Drug Targ*. **2014**, *15*, 753; h) D. K. Yadav, K. Kalani, A. K. Singh, F. Khan, S. K. Srivastava, A. B. Pant, *Curr. Med. Chem*. **2014**, *21*, 1160; i) D. K. Yadav, Saloni, P. Sharma, S. Misra, H. Singh, R. L. Mancera, K. Kim, C. Jang, M. H. Kim, H. Pérez-Sánchez, E. H. Choi, S. Kumar, *Arch. Pharm. Res*. **2017**, https://doi.org/10.1007/s12272-017-0945-7; j) D. K. Yadav, S. Kumar, Saloni, H. Singh, M. H. Kim, P. Sharma, S. Misra, F. Khan, *Drug. Des. Devel. Ther*. **2017**, *11*, 1859.

SUPPORTING INFORMATION

Additional Supporting Information may be found online in the supporting information tab for this article.

How to cite this article: Jaiswal PK, Sharma V, Kumar S, et al. Non-peptide-based new class of platelet aggregation inhibitors: Design, synthesis, bioevaluation, SAR, and *in silico* studies. *Arch Pharm Chem Life Sci*. 2018;1–17. https://doi.org/10.1002/ardp.201700349